Review of inverse analysis for indirect measurement of impact force

Hirotsugu Inoue

Department of Mechanical and Control Engineering, Tokyo Institute of Technology, 2-12-1 O-okayama, Meguro, Tokyo 152-8552, Japan; inoueh@mep.titech.ac.jp

John J Harrigan and Stephen R Reid

Department of Mechanical Engineering, UMIST, PO Box 88, Manchester M60 1QD, United Kingdom; john.j.harrigan@umist.ac.uk, steve.reid@umist.ac.uk

When dealing with the mechanics of deformable bodies, the variation of the applied force is one of the most important factors to be considered. The mechanical force acting on a body cannot be measured directly. If a body is loaded quasi-statically and if the body deforms linear-elastically, the deformation at any point of the body is proportional to the applied force. Therefore, the variation of the force can be measured indirectly by measuring the variation of the deformation. However, this principle cannot be applied when a body is subjected to an impulsive force. In this case, the propagation of stress waves inside the body cannot be neglected so that the variation of the deformation at any point of the body is no longer the same as the variation of the applied force. Therefore, impact force is much more difficult to measure than quasi-static force. In order to overcome this difficulty, inverse analysis methods to estimate variations of impact force from measured responses of a body have been studied extensively during the last two decades. This article presents a review of methods of inverse analysis for the indirect measurement of impact force. [DOI: 10.1115/1.1420194]

1 INTRODUCTION

The measurement of impact force or, more precisely, the measurement of the impact force history is a fundamental issue in impact engineering. The simplest approach to the measurement of impact force is to measure the mass and acceleration of the body subjected to impact. This approach neglects the deformation of the body and, therefore, is valid only when the body can be considered to be rigid, that is when the impact duration is much longer than the transit time of stress waves through the body. Another approach is to insert a force transducer between the colliding bodies. Since the presence of the transducer alters the contact state between the bodies, this approach can be applied only when the transducer does not affect the impact force, that is when the transducer is sufficiently smaller and softer than the colliding bodies. It is also the case that the impact force can be measured indirectly in a few special cases: for example, the impact force induced by the longitudinal impact of elastic rods can be measured using strain gauges attached to the rod and applying the theory of one-dimensional stress wave propagation (Lundberg and Henchoz [1]). However, there have been few comprehensive methods proposed which do not suffer from the limitations mentioned above, and the measurement of impact force is still difficult in many practical situations.

In order to overcome these difficulties, a new approach has been widely studied during the last two decades. The basic idea is to estimate the impact force from measurements of responses (for example, displacement, velocity, acceleration, or strain) at certain points of the body subjected to impact. The impact force is, therefore, measured indirectly in this approach. Since a variety of sensors are available to measure such responses nowadays and, in addition, the digital equipment for recording and processing data has developed remarkably in recent years, this approach is expected to become one of the most comprehensive methods for measuring impact force. In the literature, this approach is referred to as impact force identification, impact force reconstruction, inverse filtering of impact force, deconvolution of impact force etc. In this article, the various procedures and methods are categorized as inverse analyses of impact force since they are based on the solution of one or more inverse problems to infer causes (the impact force) from effects or results (the responses).

Although the measurement of the impact force history has

Transmitted by Associate Editor N Jones

ASME Reprint No AMR316 $20.00

been referred to so far, for a full understanding of the impact force it may be required to know: 1) the time history, 2) the direction, and 3) the location of the impact force. It is possible to pose problems in which each one of these three or any combination of them is required; for example, an accurate measurement of the time history is usually required in the impact testing of materials while the direction and location are major concerns in the monitoring of structures subjected to impact by foreign objects. All such problems can be regarded as inverse problems for which the solution provides information about the impact force.

Inverse problems are given attention in many fields of science and engineering (eg, Engl *et al* [2]; Groetsch [3]). There are many topics closely related to inverse analysis of impact force. One of them is the exciting force identification for vibrating machines or structures. Although the main concern there is the frequency content of the exciting force rather than the time history, techniques used for vibration problems are basically similar to those used for impact problems. Stevens [4] gave an excellent overview of this topic, which includes some early studies on inverse analysis of impact force. Other closely related topics include the source characterization of acoustic emissions or the mechanics of earthquake sources.

It is well known that inverse problems are often ill-posed in the mathematical sense, that is one of 1) the existence, 2) the uniqueness, or 3) the stability of the solution is violated. This is also the case in inverse problems for impact forces and it causes many difficulties in obtaining good estimates of the impact force. Therefore, the relaxation of the ill-posedness is a key step in establishing a comprehensive method of inverse analysis of impact force. Several mathematical techniques for achieving this have been established and some of them have been shown to be effective for inverse analysis of impact force.

In this paper, various techniques for inverse analysis of impact force including the essential difficulties, mathematical techniques and applications are summarized. The aim is to provide an overview of recent advances in order to establish a comprehensive set of methods for measuring impact force. While most of the techniques have rigorous mathematical foundations, these are not presented here in any detail, although appropriate references are provided.

2 INVERSE ANALYSIS OF TIME HISTORY

The inverse analysis of the impact force history has been studied extensively and various techniques have been developed. The most straightforward technique employed by many researchers is deconvolution. In this section, the inverse analysis of time history by means of deconvolution will be the main technique discussed. Other techniques will be mentioned briefly. It is assumed that the direction and location of the impact force are fixed and known.

2.1 Deconvolution technique

2.1.1 Basic formulation

The response of a body to an impact force can often be considered to be linearly dependent on the impact force. This is the case, for example, when the body can be considered to be linearly elastic during the impact process and when the deformation of the body can be considered to be small enough to neglect geometric nonlinearity. In such cases, the response $e(t)$ at a point of the body can be related to the impact force $f(t)$ by a linear convolution integral as

$$e(t)=\int_0^t h(t-\tau)f(\tau)d\tau, \tag{1}$$

where $h(t)$ is the impulse response function of the linear system and it is assumed that $f(t)=h(t)=e(t)=0$ for $t<0$. If the impulse response function for the chosen point on the body is known and if the response $e(t)$ is measured there, the impact force $f(t)$ can be estimated by solving the integral equation (1). Even when the body is subjected to initial motion, Eq. (1) is applicable if the response to the impact force can be separated from the total response. Thus the problem of estimating the time history can be reduced to the process of deconvolution.

2.1.2 Deconvolution in the time domain

A basic scheme for deconvolution is to discretize the integral equation (1) into algebraic equations in the time domain as

$$\boldsymbol{e}=\boldsymbol{h}\boldsymbol{f}, \tag{2}$$

where $\boldsymbol{e}$ and $\boldsymbol{f}$ are vectors composed of discrete values of $e(t)$ and $f(t)$, respectively, and $\boldsymbol{h}$ is a matrix composed of discrete values of $h(t)$, all of which are determined according to an appropriate quadrature formula. The impact force history can be estimated by solving Eq. (2) for $\boldsymbol{f}$.

The earliest work using the time domain method was that of Goodier *et al* [5]. They estimated the impact force excited by the collision of small balls onto a large block, which can be modeled as an elastic half space, from the strain measured at a point on the surface of the block. Doyle [6] also employed time domain deconvolution to estimate the impact force acting on a beam from the bending strain measured by strain gauges. In these early studies, fairly satisfactory estimates were obtained by solving Eq. (2) using Gaussian elimination. However, conventional methods such as Gaussian elimination are likely to provide severely noisy or unstable estimates in practice. The reason is that the coefficient matrix $\boldsymbol{h}$ is often ill-conditioned, that is a small perturbation in $\boldsymbol{e}$ corresponds to a quite large change in $\boldsymbol{f}$. Since experimental data of the response are always contaminated more or less with unavoidable small errors, such errors are strongly amplified by the process of deconvolution using conventional methods. Some special technique for solving Eq. (2) is required to obtain an accurate and stable estimate of the impact force.

Use of the least squares method is a common technique to improve the accuracy of the estimate. Chang and Sun [7] used a record of response of longer duration than the length of the impact force pulse to be estimated, which makes the number of equations greater than the number of unknowns in Eq. (2). They solved this least squares problem by the conjugate gradient method which is an iterative optimization technique. However, care must be taken in determining the

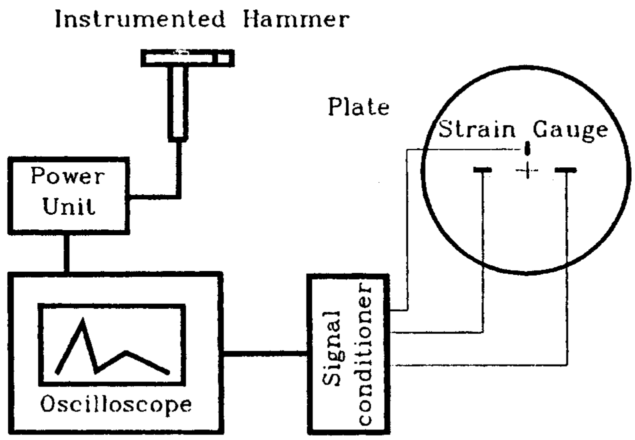

Fig. 1 Experimental setup in Wu *et al* [8]. (Reprinted with permission from the Society for Experimental Mechanics.)

number of iterations because too many iterations might provide an unstable estimate by the same reason as in conventional methods. Unfortunately, no discussion on the iteration number was given by Chang and Sun.

Wu *et al* [8] also utilized the least squares method, in which several records of responses measured at multiple locations were considered simultaneously. In addition, in order to obtain a stable estimate, they imposed the physical constraint that the impact force must be non-negative. This means that the impact force induced by collision of bodies is always compressive or zero (except when the colliding bodies stick to each other). This least squares problem with the non-negativity constraint was solved by an iterative optimization technique called the gradient projection method. An experiment to measure the impact force applied to an aluminum plate with an impact hammer was conducted as shown in Fig. 1. The estimate obtained from three strain records by this technique (Fig. 2) matches the direct measurement by the impact hammer better than those obtained from each strain record (Fig. 3). The effectiveness of the non-negativity constraint was demonstrated by Yen and Wu [9] as shown in Fig. 4 which was obtained by conducting an experiment for a

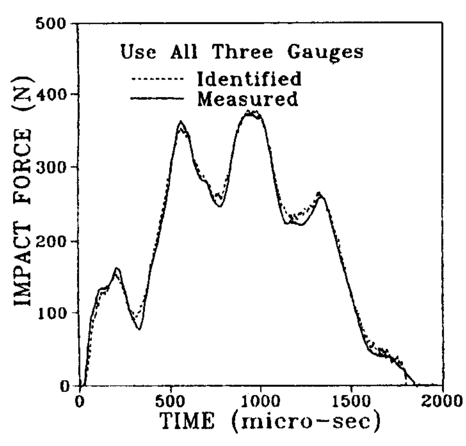

Fig. 2 Impact force estimated from three strain records [8]. (Reprinted with permission from the Society for Experimental Mechanics.)

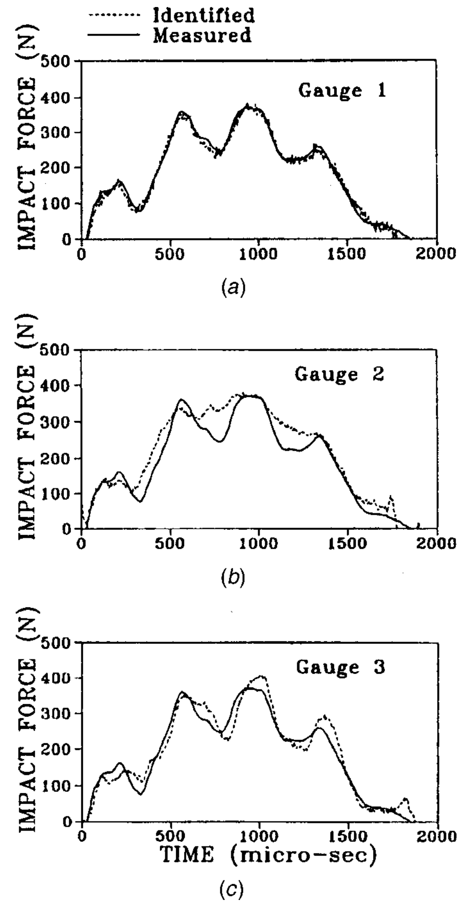

Fig. 3 Impact forces estimated from each strain record [8]. (Reprinted with permission from the Society for Experimental Mechanics.)

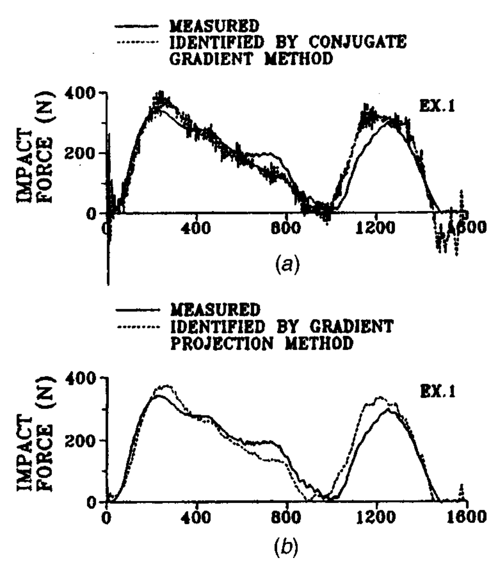

Fig. 4 Impact force estimated by: *a*) the conjugate gradient method (without non-negativity constraint) and *b*) the gradient projection method (with non-negativity constraint); the solid curves represent the forces measured directly by the impact hammer [9].

rectangular plate in a similar manner to Fig. 1. It can be seen that the estimate obtained by imposing the non-negativity constraint matches well to the direct measurement. In their subsequent paper, Wu *et al* [10] performed a numerical simulation of impact of a laminated plate and showed that their technique improves the quality of the estimate even when the response records are very noisy (the signal-to-noise ratio was set to two). They also discussed the number of iterations of the gradient projection method and showed that too many iterations cause the estimate to become unstable. A criterion for the iteration number which results in an accurate and stable estimate was given. Unfortunately, the criterion is not fully quantitative but has qualitative features. Their technique was also applied to impact of sandwich panels (Tsai *et al* [11]).

Various mathematical techniques classed as regularization techniques (eg, Engl *et al* [2]; Groetsch [3]) are available for relaxing the ill-conditioning. Truncated Singular Value Decomposition (TSVD) is one of the simplest techniques among others (eg, Groetsch [3]; Hansen [12]). The singular value decomposition of a matrix $\boldsymbol{h}$ is defined as

$$\boldsymbol{h}=\boldsymbol{U}\boldsymbol{\Sigma}\boldsymbol{V}^H, \tag{3}$$

where $\boldsymbol{U}$ and $\boldsymbol{V}$ are unitary matrices ($\boldsymbol{U}^H\boldsymbol{U}=\boldsymbol{V}^H\boldsymbol{V}=\boldsymbol{I}$), Σ is a diagonal matrix, and superscript H denotes the conjugate transpose of a matrix. The diagonal elements σ_i of $\boldsymbol{\Sigma}$ are non-negative real numbers called the singular values of $\boldsymbol{h}$. The number of non-zero singular values is called the rank of $\boldsymbol{h}$. The minimum-norm least-squares solution of Eq. (2) is given by

$$\hat{\boldsymbol{f}}=\boldsymbol{h}^\dagger\boldsymbol{e}=\boldsymbol{V}\boldsymbol{\Sigma}^\dagger\boldsymbol{U}^H\boldsymbol{e}, \tag{4}$$

where $\boldsymbol{h}^\dagger$ denotes the Moore-Penrose generalized inverse of $\boldsymbol{h}$ and $\boldsymbol{\Sigma}^\dagger$ is a diagonal matrix whose elements are the reciprocals of σ_i (the reciprocal of zero is replaced with zero). If there are singular values much smaller than the largest one, their reciprocals become very large and cause amplification of small errors involved in $\boldsymbol{e}$, which results in instability of the solution $\hat{\boldsymbol{f}}$. The idea of the TSVD is to reduce the rank of $\boldsymbol{h}$, that is to replace small singular values with zeros so as to prevent the amplification of errors. This can be considered as ignoring information of low quality. It is important to determine appropriately the degree of regularization, ie, the number of singular values to be replaced with zeros. Tanaka and Ohkami [13] employed the TSVD in estimating the impact force acting on a pipe from its response measured by an accelerometer. They obtained estimates of the impact force at various values of the rank as shown in Fig. 5. The estimate is severely noisy when the rank is 130 that is when none of the singular values is replaced with zero. As the rank is reduced, the estimate becomes more stable and approaches the direct measurement obtained by an impact hammer. At the rank of 72, the mean square discrepancy between the estimate and the direct measurement becomes minimum. However, as the rank is reduced further, the estimate becomes inaccurate and approaches the data which were obtained by calibration for determining $\boldsymbol{h}$ experimentally. In Figs. 5*d* and 5*e*, estimated data coincide with calibration data. They compared two evaluation criteria, the Akaike information criterion and the

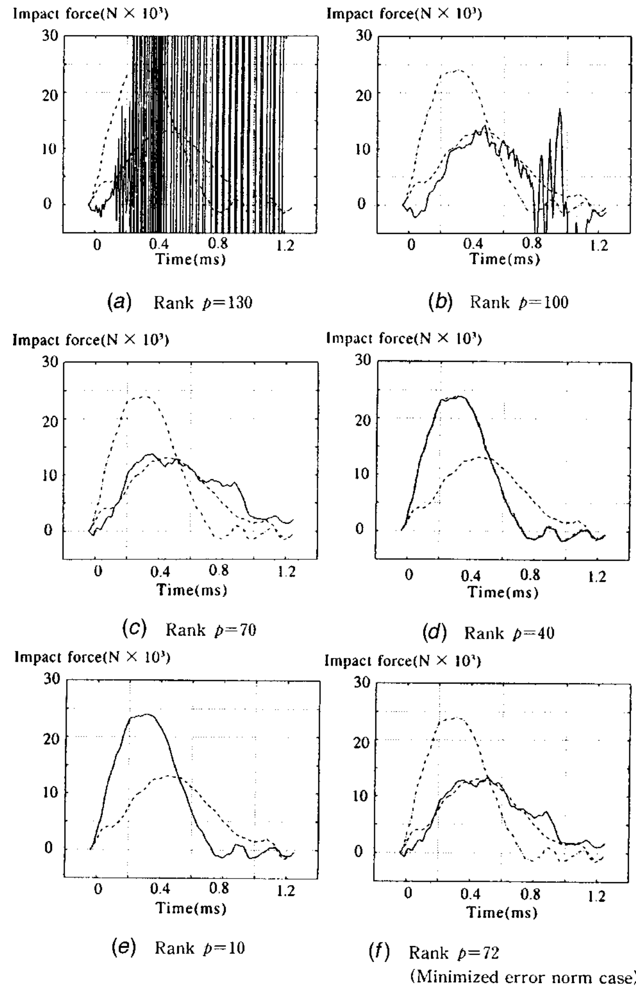

Fig. 5 Estimates of an impact force at various values of the rank; solid curve: estimated data, broken curve: directly measured data, dotted curve: calibration data [13]. (Reprinted with permission from the Japan Society of Mechanical Engineers.)

penalty quadratic form, in order to determine the appropriate degree of regularization. It was shown that this is achieved at the rank of 73 where the magnitude of the penalty quadratic form becomes minimum.

Another well known technique of regularization is Tikhonov regularization which imposes an additional constraint on the solution to be obtained (eg, Engl *et al* [2]; Groetsch [3]). The simplest form of Tikhonov regularization for the problem represented by Eq. (2) is to find a solution $\boldsymbol{f}_\lambda$ so as to minimize the functional

$$\|\boldsymbol{h}\boldsymbol{f}_\lambda-\boldsymbol{e}\|^2+\lambda\|\boldsymbol{f}_\lambda\|^2, \tag{5}$$

where $\|\cdot\|$ denotes the Euclidean norm and the parameter λ is a positive constant called the regularization parameter. The functional (5) indicates that Tikhonov regularization is based on the least squares method (the first term) with an additional constraint on the norm of the solution (the second term). This constraint makes the solution stable at the expense of allowing the original Eq. (2) not to be satisfied perfectly in the least squares sense. The solution $\boldsymbol{f}_\lambda$ is unstable if λ is too small while it becomes inaccurate if λ is too large. Therefore, the parameter λ should be determined appropriately in order to obtain an accurate and stable solution. The solution which minimizes the functional (5) is given by

$$\hat{\boldsymbol{f}}_\lambda = \boldsymbol{V}\boldsymbol{\Sigma}_\lambda^\dagger \boldsymbol{U}^H \boldsymbol{e}, \tag{6}$$

where $\boldsymbol{\Sigma}_\lambda^\dagger$ is a diagonal matrix whose elements are expressed as $\sigma_i/(\sigma_i^2+\lambda)$ instead of $1/\sigma_i$ in $\boldsymbol{\Sigma}^\dagger$. Unfortunately, to the authors' knowledge, no researcher has applied Tikhonov regularization to time domain deconvolution for estimating the impact force. However, since it is one of the standard techniques for solving ill-conditioned problems, it is worth mentioning here. A comparison of Tikhonov regularization with the Wiener filter described later is interesting.

Other methods using deconvolution in the time domain have been provided by Hojo *et al* [14] and Zhu and Lu [15].

2.1.3 Deconvolution in the frequency domain

Another basic scheme for deconvolution is to transform the convolution in the time domain into a multiplication in the frequency domain using Fourier transforms resulting in

$$E(\omega) = H(\omega)F(\omega), \tag{7}$$

where the symbols in uppercase denote the Fourier transforms of the corresponding ones in lowercase. If the transfer function $H(\omega)$, which is the Fourier transform of the impulse response function, is known in advance, the impact force can be estimated by evaluating the Fourier transform of the measured response, finding $F(\omega)$ from Eq. (7) and evaluating its inverse. It is well known that the use of Fast Fourier Transforms (FFT) makes the computational task for deconvolution in the frequency domain much less than that for deconvolution in the time domain. However care must be taken to reduce errors due to numerical discretization and truncation of the Fourier integral when applying the FFT algorithm.

One of the earliest uses of frequency domain deconvolution was made by Holzer [16] who corrected the force-time records of high-speed compression tests obtained by short load cells. He pointed out that high frequency noise tends to be amplified by the division $E(\omega)/H(\omega)$ and hence that it is necessary to employ low pass filters. As discussed later, this amplification of noise is due to the ill-conditioned nature of deconvolution. Although low-pass filtering is certainly a simple and effective technique for removing high frequency noise, it also removes information in the high frequency range which is important in some cases. For example, in dynamic crushing tests of materials, a steep peak in the loading history is an important factor when characterizing such materials. Careless application of a low-pass filter might distort such a peak. This disadvantage of the low-pass filter may be overcome by using the Wiener filter described later.

Doyle [17] applied frequency domain deconvolution to estimating the impact force acting on beams from the bending strain measured by a strain gauge. Comparing the results with those obtained in his preceding work in which he used time domain deconvolution [6], Doyle claimed that frequency domain deconvolution is preferable mainly because of its simplicity. He and his co-workers subsequently applied

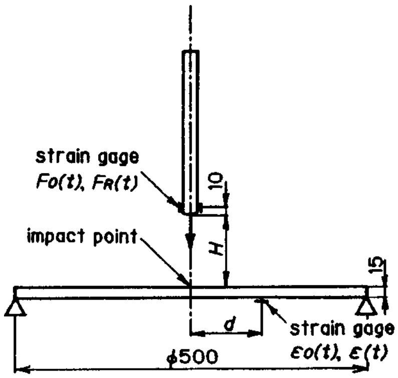

Fig. 6 Impact on a steel plate with a steel rod [24].

the frequency domain deconvolution to estimate the time histories of impact forces acting on various structural components (Doyle [18–20], Martin and Doyle [21], Rizzi and Doyle [22]). In addition, he showed that padding the response data with zeros before deconvolution is effective in reducing the error due to discretization of the Fourier integral. Hojo *et al* [14] also compared the frequency domain method to the time domain method and demonstrated that there are very few qualitative differences between the estimates obtained by these two methods.

Fourier transforms are defined by infinite integrals, but truncation of data to a finite length is necessary for practical computations. This truncation introduces a discontinuity at the end of the data and causes errors which are termed *leakage*. The leakage can be reduced by applying an exponential window $\exp(-\gamma t)$ to the data, where γ is a positive constant. Exponential windowing introduces a linear damping which decreases the severity of the discontinuity. Inoue *et al* [23,24] adopted exponential windowing to estimate impact forces on a beam and a plate from the bending strain measured by a strain gauge. For the case of impact on a steel plate with a steel rod (Fig. 6), a satisfactory estimate was obtained at an appropriate value of γ (Fig. 7). The appropriate value of γ is empirically known to be about $2\pi/T$ if the signal to be processed is free from noise (Wilcox [25]; Inoue *et al* [26]), where T is the time duration of the signal to be processed. If the signal is contaminated with noise, however, a smaller value is recommended in order to avoid the exponential amplification of noise [Fig. 7*c*]. Hojo *et al* [14] also pointed out that exponential windowing is necessary to obtain a good estimate by the frequency domain method. Note that the equivalence of convolution in the time domain to multiplication in the frequency domain is violated if other types of window such as a Hanning window (usually used for evaluating the power spectrum) are used. Nakao *et al* [27] applied a Hanning window, but unfortunately obtained highly distorted estimates.

In fact, a Fourier transform with an exponential window is equivalent to the Laplace transform and hence numerical inversion to obtain $f(t)$ from $F(\omega)$ by FFT can be regarded as a numerical inverse Laplace transformation ([25], [26]). Since the inverse Laplace transform is a typical ill-posed problem (eg, Engl *et al* [2]), care must be taken to obtain a

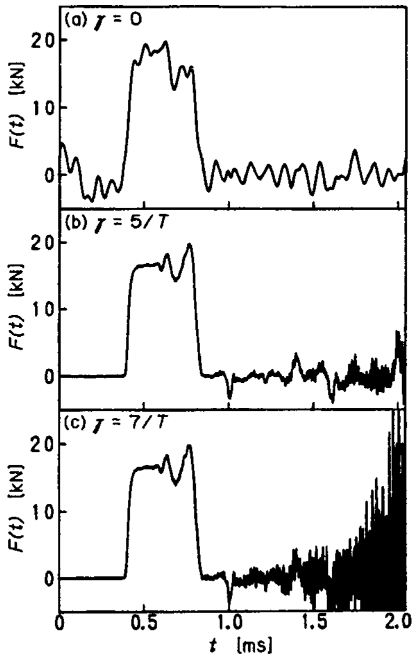

Fig. 7 Impact force estimated from bending strain of the plate [24].

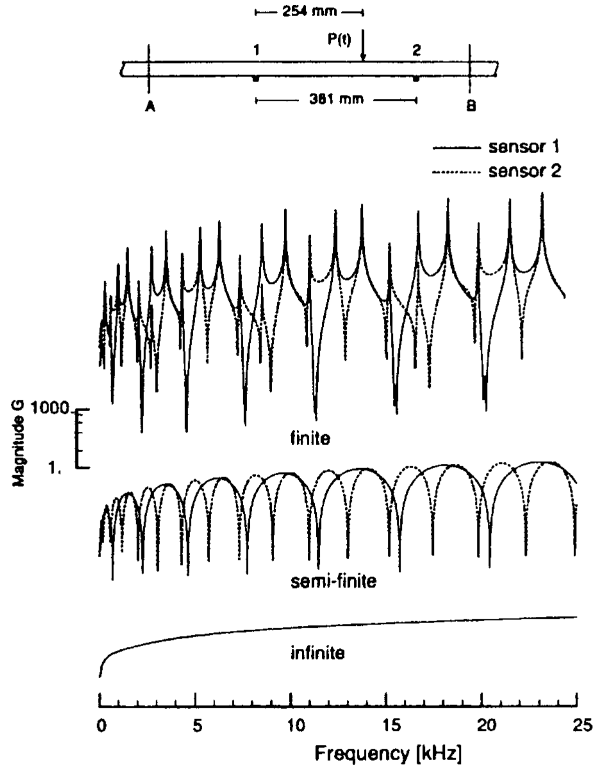

Fig. 8 Moduli of transfer functions for simple beam structures [21]. (Reprinted with permission from Elsevier Science.)

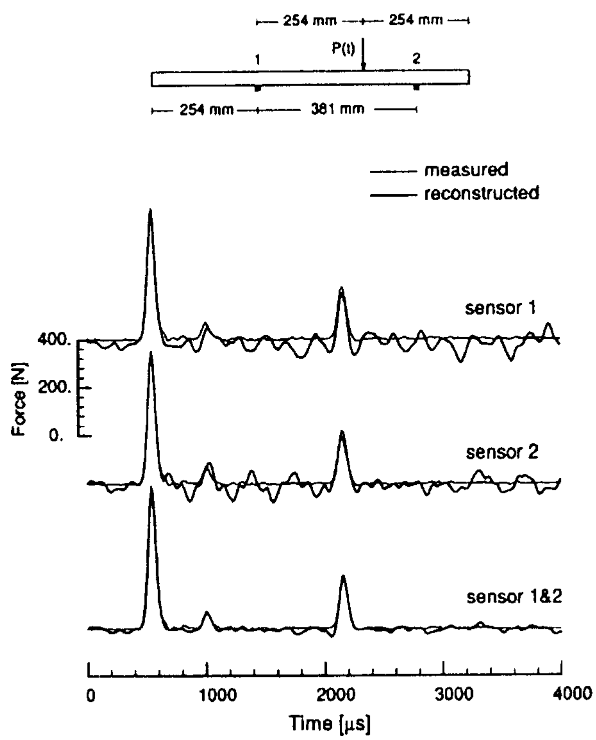

Fig. 9 Impact forces on the finite beam estimated from each record and from two records of responses [21]. (Reprinted with permission from Elsevier Science.)

good result. Inoue *et al* [28] applied Tikhonov regularization to numerical Laplace inversion to improve the accuracy of the estimate. It was shown that Hansen's L-curve method [12,29] is effective in determining an optimal value of the regularization parameter.

The least squares method considering responses measured at multiple locations is effective for improving the accuracy of the estimate also in the frequency domain method. The benefit of the use of multiple responses can be explained as follows. The modulus of the transfer function can become very small at a certain frequency and at a certain location at which the response is measured. In such a case, the response at that location contains little information about the impact force at that frequency. However, the responses at other locations may contain sufficient information about the impact force at the same frequency because the transfer function varies with the location. Therefore, the use of responses measured at more than two locations is beneficial in compensating for the lack of information at each location. Inoue *et al* [30] applied the least squares method for estimating the impact force applied to a GFRP plate from strain responses measured at multiple locations. Martin and Doyle [21] illustrated the benefit clearly by a simple example of impact on beams as shown in Figs. 8 and 9. The anti-resonant frequencies at location 1 are different from those at location 2. As a result, the impact force estimated from two records measured at locations 1 and 2 is much better than those estimated from each record.

An explicit consideration of the small noise involved in the response data makes the difficulty of accurate deconvolution clearer. Suppose that the measured response $y(t)$ is the sum of the true response $e(t)$ and a small noise $n(t)$. If $y(t)$ is used as an approximation to $e(t)$, the estimate of the impact force in the frequency domain is given as

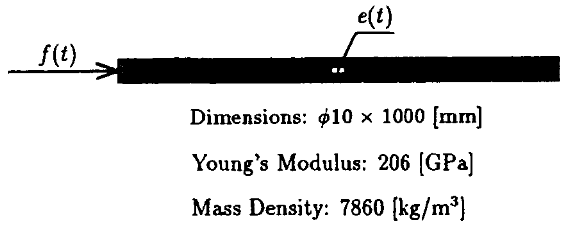

Fig. 10 Longitudinal impact of a slender rod [31].

$$\hat{F}(\omega)=\frac{Y(\omega)}{H(\omega)}=\frac{E(\omega)}{H(\omega)}+\frac{N(\omega)}{H(\omega)}. \tag{8}$$

If $|H(\omega)|$ is very small at a certain frequency, $|E(\omega)|$ is also very small and hence the second term of Eq. (8) becomes dominant over the first term at that frequency. Then the noise $N(\omega)$ is considerably amplified due to the division by the small value $|H(\omega)|$ and, as a result, the estimate $\hat{F}(\omega)$ becomes very noisy and far from the true impact force $F(\omega)$.

Inoue *et al* [31] adopted the Wiener filter to overcome this difficulty. The Wiener filter is an optimal inverse system to minimize the mean square error of the estimate. If the noise $n(t)$ is uncorrelated with $f(t)$ and $e(t)$, the non-causal Wiener filter is given by

$$G(\omega)=\frac{S_{yf}(\omega)}{S_{yy}(\omega)}=\frac{H^*(\omega)}{|H(\omega)|^2+S_{nn}(\omega)/S_{ff}(\omega)}, \tag{9}$$

where $S_{yf}(\omega)=Y^*(\omega)F(\omega)$ is the cross-spectrum between $y(t)$ and $f(t)$, and the superscript $*$ denotes the complex conjugate. The estimate in the frequency domain is given as

$$\tilde{F}(\omega)=G(\omega)Y(\omega)=\frac{H^*(\omega)[E(\omega)+N(\omega)]}{|H(\omega)|^2+S_{nn}(\omega)/S_{ff}(\omega)}. \tag{10}$$

If there is no noise (that is $N(\omega)=0$), the estimate $\tilde{F}(\omega)$ becomes $E(\omega)/H(\omega)$ which is the true impact force $F(\omega)$. On the other hand, if the noise is very large that is $|N(\omega)| \to\infty$, the estimate $\tilde{F}(\omega)$ tends to zero. The amplification of noise is suppressed to an appropriate degree depending on the signal to noise ratio $S_{ff}(\omega)/S_{nn}(\omega)$. The effectiveness of the Wiener filter was demonstrated by numerical simulation in which the impact force acting on a rod was estimated from its strain response (Fig. 10) [31]. Each signal used in this simulation was contaminated artificially with random noise having amplitude 1% of the maximum value of the signal. While the estimate obtained by direct deconvolution (Fig. 11*a*) suffers oscillations due to the amplification of small noise, such oscillations are successfully suppressed by applying the Wiener filter (Fig. 11*b*). The effectiveness of the Wiener filter was also verified experimentally through the measurement of impact force on a cantilever (Kishimoto *et al* [32]).

Some additional comments concerning the Wiener filter may be of interest. An important point is that the Wiener filter is not equal to the reciprocal of the true transfer function. This means that a precise prediction of the transfer function does not always lead to an accurate estimate of the impact force. Another interesting point is the similarity between the Wiener filter and Tikhonov regularization (Bertero *et al* [33]). Roughly speaking, the Fourier transformation and the inversion correspond to the matrices $\boldsymbol{U}^H$ and $\boldsymbol{V}$ in Eq. (6) respectively. In addition, the factor $S_{nn}(\omega)/S_{ff}(\omega)$ in Eq. (9) corresponds to the regularization parameter λ in $\sigma_i/(\sigma_i^2+\lambda)$ which is the diagonal element of the matrix $\boldsymbol{\Sigma}_\lambda^\dagger$ in Eq. (6). When it is difficult to evaluate the factor $S_{nn}(\omega)/S_{ff}(\omega)$ as a function of the frequency, an appropriate constant can be used in place of this factor as suggested by Martin and Doyle [21] and Doyle [34].

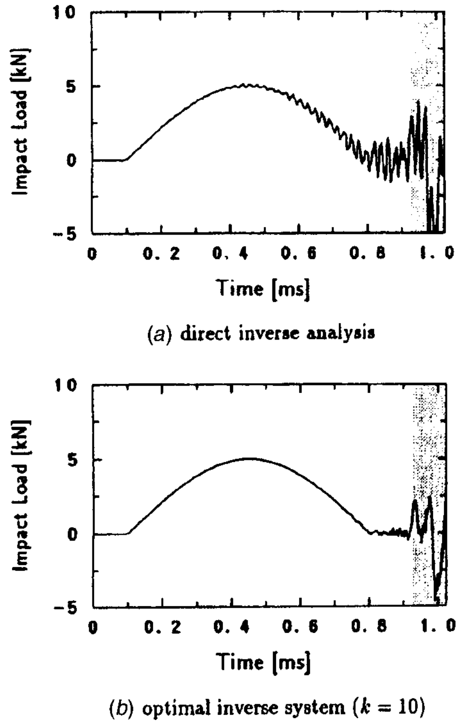

Fig. 11 Impact force estimated by: *a*) direct deconvolution and *b*) the Wiener filter [31].

Other work using deconvolution in the frequency domain was performed by Whiston [35], Jordan and Whiston [36], Kishimoto *et al* [37], Inoue *et al* [38], Bateman *et al* [39], Kim and Lyon [40], Lin and Bapat [41], and McCarthy and Lyon [42].

2.1.4 Deconvolution using wavelets

The use of wavelets for deconvolution has become possible with the recent development of the mathematical theory for wavelet transforms (eg, Daubechies [43]). One of the most important features of the wavelet transform is that a function is expressed as a linear combination of wavelets whose durations are usually finite in time. This is in contrast to the Fourier transform in which a function is expressed by a linear combination of sinusoidal functions having infinite durations.

Doyle [34] developed a deconvolution method using wavelets for estimating impact force. The impact force is expressed as a linear combination of wavelets which are produced by shifting a basic wavelet in time. This expression seems quite reasonable since impact force has a finite duration in many cases. On the other hand, the response is expressed as a linear combination of responses to the wavelet forces. Substituting these expressions into the convolution integral and applying the least squares method, he obtained a system of algebraic equations to be solved for the coefficients of the wavelet forces.

Doyle used wavelets produced only by shifting the basic wavelet. However, according to the theory of wavelets (eg, Daubechies [43]), it would be interesting to make an attempt to use wavelets produced not only by shifting, but also by dilating the basic wavelet in time.

2.1.5 Identification of the transfer function

The impulse response function or its Fourier transform, the transfer function, is necessary for estimating the impact force history by the deconvolution technique. Since the quality of the transfer function significantly affects the quality of the estimate of the impact force, a discussion of how to obtain the transfer function is important. There are three approaches to obtain the transfer function: 1) prediction by theoretical analysis, 2) identification by experimental analysis, and 3) identification by numerical analysis, each of which has some advantages and disadvantages in estimating accurately the impact force.

The prediction by theoretical analysis requires precise modeling of the structure under consideration which must include all factors such as shape, size, material properties, boundary conditions, etc. Even if there are slight errors in the model and hence in the prediction of the transfer function, the estimate of the impact force might become very poor because of the ill-posedness of the inverse problem. Nevertheless some compromises to simplify the model are required at the expense of the accuracy of the estimate of the impact force since too precise modeling makes the theoretical analysis difficult. Whiston [35] and Jordan and Whiston [36] predicted the transfer function of beams according to Timoshenko theory, in which they considered an infinite beam, so ignoring the reflections from supports. Doyle and his coworkers also ignored reflections from boundaries in predicting transfer functions for beams [6,17], plates [18], orthotropic plates [19], plates subjected to in-plane impact [22], and bimaterial beams [20]. Ignoring these reflections is justified only when the wave components reflected from the boundaries are clearly separated from those arriving directly from the impact site in the record of the measured response. Doyle [17] proposed countermeasures to compensate for ignoring the reflections but they are not definitive. Goodier *et al* [5], Lin and Bapat [41], Tsai *et al* [11], Wu *et al* [8,10], and Yen and Wu [9,44] also predicted transfer functions by theoretical analyses.

In experimental identification, the transfer function is basically identified by conducting a calibration test: that is applying an impact force to the structure, measuring both the impact force and the response and deconvolving the impact force from the response basically in the same manner as estimating the impact force from the response. Experimental identification is quite different from analytical prediction in the sense that *all factors* can be taken into account without any modeling in so far as they are linear. Here *all factors* include, not only the true transfer function of the structure under consideration, but also the dynamic response characteristics of the equipment used for measuring the response. Even slight errors in the experimental setup (such as misalignment of strain gauges for measuring the strain response) can be compensated for because they are incorporated in the transfer function. On the other hand, the impact force in the calibration test must be measured as accurately as possible because the accuracy of the impact force estimated by deconvolution can never be better than the accuracy of the impact force measured in the calibration test. Inoue *et al* used slender rods with attached strain gauges as the impactor in the calibration test to identify the transfer functions of beams [23,32], plates [24,30], and a Charpy testing machine [38,45]. A similar method was adopted by Hojo *et al* [14] who utilized the method developed by Lundberg and Henchoz [1]. Kishimoto *et al* [37] used a steel ball instrumented with an accelerometer. Impact hammers (typically used for experimental modal analysis) were employed by Bateman *et al* [39], Zhu and Lu [15], Kim and Lyon [40], McCarthy and Lyon [42], and Tanaka and Ohkami [13].

The identification of the transfer function from experimental data has many difficulties similar to those encountered in estimating the impact force since it is also an inverse problem. Small errors involved in the calibration data cause significant errors in the transfer function and, as a result, makes the estimate of the impact force very poor. Several techniques applied to the estimation of the impact force are also effective for the identification of the transfer function. In particular, exponential windowing is effective for obtaining a transfer function which provides a stable estimate of the impact force. If the transfer function has non-minimum-phase zeros which are not true ones, but ones introduced in error by the identification process, then the deconvolution process to estimate the impact force becomes unstable (eg, Kim and Lyon [40], McCarthy and Lyon [42]). Exponential windowing is also effective in avoiding the introduction of such non-minimum-phase zeros [46].

Inoue *et al* [45] compared five methods of identifying the transfer function and showed that one of them provides a good estimate of the impact force. The method is to identify the transfer function from many sets of data obtained by repeating the calibration test according to the equation

$$\hat{H}(\omega)=\frac{\sum_k Y_k^*(\omega)Y_k(\omega)}{\sum_k Y_k^*(\omega)X_k(\omega)}, \tag{11}$$

where $X_k(\omega)$ and $Y_k(\omega)$ denote the Fourier transforms of the impact force and the response measured in the kth calibration test. In their subsequent paper (Inoue *et al* [31]), it was shown that the transfer function identified by Eq. (11) is a good approximation to the reciprocal of the Wiener filter $1/G(\omega)$. It is interesting that the factor $S_{nn}(\omega)/S_{ff}(\omega)$ in Eq. (9), which is a key factor in obtaining an accurate and stable estimate of the impact force, is determined automatically.

In some practical applications such as the diagnosis of commercial products, the transfer function identified for a particular sample is used for the diagnosis of a number of nominally identical products. However, there always exists variability in the transfer functions of individual products. Kim and Lyon [40] and McCarthy and Lyon [42] considered the effect of this variability on the estimate of the impact force. The transfer function and the response can have non-minimum-phase zeros which ideally cancel each other. If the cancellation is imperfect because of the variability of the transfer function, then the non-minimum-phase zeros cause instability in the deconvolution process. They proposed a technique named minimum-phase processing in which the instability is avoided by using only the minimum-phase components of the transfer function.

Some techniques in which deconvolution is not required for identifying the transfer function have also been proposed. If the duration of the impact force in the calibration test is much shorter than that of the impact force to be estimated, then the response in the calibration test can be a good approximation to the impulse response function. Holzer [16] and Chang and Sun [7] used a small ball as the impactor in the calibration test to produce an impact force with a very short duration. Another technique is proposed by Wu *et al* [8]. They derived a relationship

$$\int_0^t e_c(t-\tau)f(\tau)d\tau=\int_0^t e(t-\tau)f_c(\tau)d\tau, \tag{12}$$

where the subscript c denotes the data obtained by the calibration test. Since $e(t)$, $e_c(t)$ and $f_c(t)$ are given, the above equation can be solved for $f(t)$ by the gradient projection method with the non-negativity constraint mentioned above. It is interesting that no explicit deconvolution is required not only for the identification of the transfer function, but also for the estimation of the impact force. The validity of this technique was demonstrated by experiments on impact of a laminated plate [8]. Further verification of this technique was conducted by Wu *et al* [47] where impacts on rods and a honeycomb-cored sandwich panel were considered.

When it is difficult to conduct a calibration test, numerical analysis is a good alternative for identifying the transfer function of actual structures. It is important to check the validity of the numerical analysis much more carefully than usual because the estimate of the impact force may become very poor even if there are slight errors in the transfer function. Harrigan *et al* [48] employed the FEM to identify the transfer function of pressure bars used in high-speed compression tests of cellular materials.

2.2 Other techniques

2.2.1 State variable formulation

The input-output relationship of a linear system can be expressed also by a linear differential equation. The differential equation can generally be reduced to a set of first-order differential equations in terms of state variables as follows (eg, DeRusso *et al* [49], Trujillo and Busby [50]):

$$\dot{\boldsymbol{x}}(t)=\boldsymbol{K}\boldsymbol{x}(t)+\boldsymbol{T}\boldsymbol{f}(t), \tag{13}$$

$$\boldsymbol{e}(t)=\boldsymbol{Q}\boldsymbol{x}(t), \tag{14}$$

where $\boldsymbol{x}(t)$, $\boldsymbol{f}(t)$ and $\boldsymbol{e}(t)$ are vectors composed of state variables, inputs and outputs of the system, respectively, and $\boldsymbol{K}$, $\boldsymbol{T}$ and $\boldsymbol{Q}$ are matrices determined by the properties of the system.

Hollandsworth and Busby [51] adopted the state variable formulation and considered the minimization of the following expression:

$$\sum_k \left[\|\boldsymbol{d}(k\Delta t)-\boldsymbol{Q}\boldsymbol{x}(k\Delta t)\|^2+b\|\boldsymbol{f}(k\Delta t)\|^2\right], \tag{15}$$

where Δt is the time interval for discretization, $\boldsymbol{d}(k\Delta t)$ is the measurement for $\boldsymbol{e}(k\Delta t)$ and b is an appropriate constant. Note that minimization of the above functional is equivalent to Tikhonov regularization. They described a general method to solve this problem using the dynamic programming technique which is often used for solving optimal control problems. They demonstrated its validity by estimating the impact force acting on a cantilever from its accelerations [51]. Busby and Trujillo [52] applied a similar method for estimating the impact force acting on a plate, in which the regularization parameter b was optimized by the method of generalized cross-validation (eg, Engl *et al* [2]; Hansen [12]). These techniques are summarized in a monograph by Trujillo and Busby [50].

The advantage of this technique may be that various sophisticated techniques developed in the field of control engineering are available. Unfortunately, this technique requires that the differential equations describing the system can be formulated adequately, which might be difficult in many practical cases.

2.2.2 Sum of weighted accelerations

Bateman *et al* [39,53] proposed a technique termed the Sum of Weighted Accelerations Technique (SWAT) to measure the impact force and moment acting on structures with free boundary conditions. If the body subjected to impact can be considered as a rigid body, the impact force may be obtained by measuring the mass and acceleration of the body. SWAT is something of an extension of this simple idea for application to deformable bodies. In SWAT, the impact force $f(t)$ and moment $M(t)$ are estimated by

$$f(t)=\sum_k W_k a_k(t), \tag{16}$$

$$M(t)=\sum_k G_k a_k(t), \tag{17}$$

where $a_k(t)$ is the measured acceleration at the kth location of the body and W_k and G_k are weighting factors having the units of mass and first-moment-of-mass, respectively. These factors are determined so as to eliminate the elastic response of the body on the basis of modal analysis. They applied SWAT to measure the impact force applied to real structures, a scale model nuclear transportation cask and an energy-absorbing nose used for the delivery of bombs. They also compared SWAT with the deconvolution technique and concluded that both techniques provided satisfactory results [39].

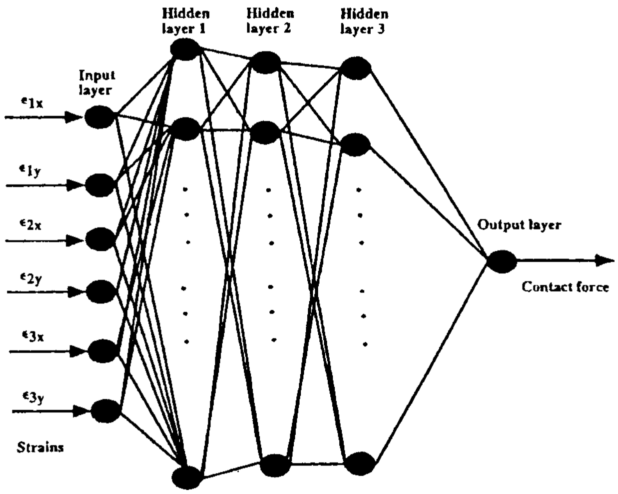

Fig. 12 A back-propagation neural network for estimation of impact force [54]. (Reprinted with permission from Elsevier Science.)

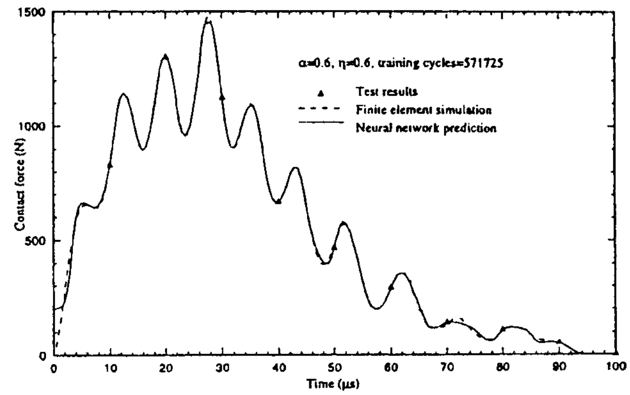

Fig. 13 Impact force history estimated by a neural network [54]. (Reprinted with permission from Elsevier Science.)

The main disadvantage of SWAT is the difficulty of determining the weighting factors. However, the post-processing of the measured acceleration is very simple which is the most favorable feature of this technique.

2.2.3 *Neural network*

Neural networks are systems composed of a large number of interconnected parallel processing units. Each unit receives inputs from other units and sends a common output to other units. The input-output relationship of each unit is described by some simple rule. Although various network architectures can be constructed, one of the most popular ones is a back-propagation network having a multilayered architecture as shown in Fig. 12. It is made up of an input layer, one or more intermediate (*hidden*) layers and an output layer. The input of each unit in a layer is a simple function of the weighted sum of outputs from units in the previous layer. The weights of each unit are determined by the *training* procedure: for a given set of many input-output pairs of a network, the weights are adjusted so as to match the outputs derived from the true inputs to the corresponding true outputs. An algorithm called error back-propagation is employed for the training procedure.

Chandrashekhara *et al* [54] applied the neural network technique to estimating the impact force acting on composite plates from their bending strains. A back-propagation network with one input layer (six units), three hidden layers (20 or 10 units), and one output layer (one unit) was used (Fig. 12). The inputs to the network are in-plane normal strains at three different locations of a plate while the output is the impact force. This network was trained using 180 input-output pairs generated by finite element analyses. After the training, several input-output pairs which were not used in the training were generated for testing the performance of the network. An example of the test result is shown in Fig. 13. It can be seen that the estimate obtained by the network is in good agreement with the result of the finite element analysis.

The most important advantage of the neural network technique is that it can be applied even when the relationship between the impact force and the response is nonlinear, although some difficulties may arise when there are strong nonlinearities. Another advantage is that the estimation procedure is very simple once the training process is completed. On the other hand, the architecture and parameters of the network should be determined appropriately so as to obtain an accurate estimate of impact force, which requires experience. It is also a drawback of the neural network technique that a large number of data sets are required to train the network adequately.

2.3 Practical applications

A typical application of inverse analysis of the impact force history is the measurement of impact forces in the impact testing of materials. An accurate measurement of impact force is necessary in order to evaluate mechanical properties of materials adequately. Some examples are discussed here to demonstrate the importance of accurate measurement of impact force.

2.3.1 *Instrumented Charpy impact test*

The Charpy impact test is one of the most classical methods for evaluating the toughness of materials under impact loading. Unfortunately, in its original form, it gives only the energy required to break the specimen by the pendulum hammer. In order to obtain more detailed information relevant to the mechanical behavior of the specimen during impact, instrumentation of the Charpy testing machine has been widely studied by many researchers. The measurement of the impact force acting on the specimen is one of the most important issues. The impact force is usually measured by attaching some sensor to the head of the hammer (the tup). However, since the hammer has a somewhat complicated shape from the view point of the propagation of stress waves, the signal detected by the sensor usually experiences contributions from multiple reflections of stress waves within the hammer and, therefore, does not represent the true impact force. Several attempts to obtain an accurate measurement of the impact force have been made but they are not definitive.

Inoue *et al* [38,45] applied inverse analysis to this problem. First, a steel rod which was placed horizontally in the place of the specimen was impacted longitudinally by the

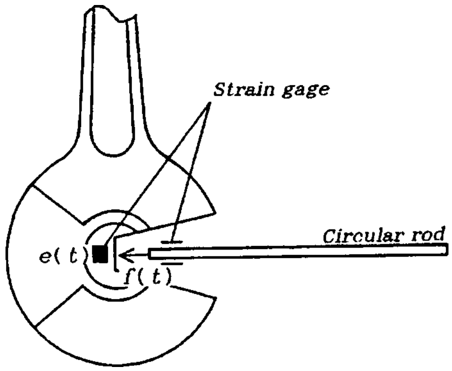

Fig. 14 Impact of a rod with the hammer of the Charpy testing machine: calibration test [45].

hammer to conduct a calibration test (Fig. 14). The impact force acting between the tup and the rod was measured by using strain gauges attached to the rod while the strain response of the hammer was also measured by strain gauges attached to the tup as shown in Fig. 15. It can be seen that the impact force pulse is almost rectangular while the strain response has a slow sinusoidal vibration superposed on the rectangular pulse. This sinusoidal vibration is caused by wave propagation within the hammer. The transfer function between the impact force and the strain response was identified according to Eq. (11). Then testing of a PMMA specimen was conducted and the strain responses of the hammer were measured as shown in Fig. 16. Frequency domain deconvolution of the transfer function from these strain response records resulted in estimates of the impact forces as shown in Fig. 17. The slow sinusoidal vibration seen in the strain responses was successfully removed. The impact forces are oscillatory before reaching their maximum values, which is due to mechanical interaction between the tup and the specimen. It should be emphasized that this oscillation does not correspond to wave propagation within the hammer

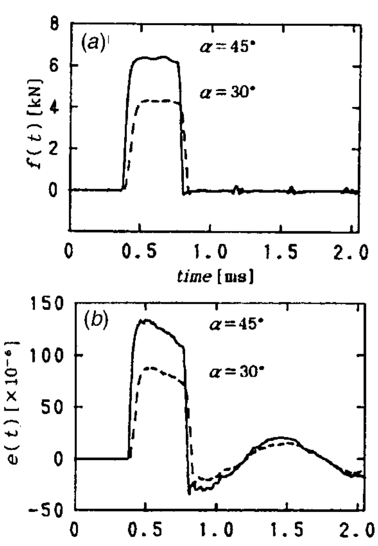

Fig. 15 Results of the calibration test: *a*) impact force between the tup and the rod, *b*) strain response of the hammer (α: release angle of the hammer) [45].

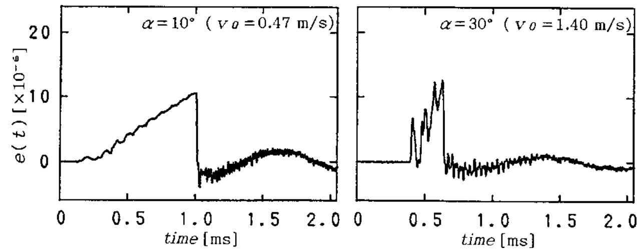

Fig. 16 Strain responses of the hammer in the testing of PMMA specimen [45].

and, therefore, must not be neglected in order to understand the mechanical behavior of the specimen correctly.

The same technique was further applied to measuring impact fracture toughness of materials using the Charpy testing machine and pre-cracked specimen [55].

2.3.2 Dynamic compression test

Dynamic compression tests are often conducted for evaluating the performance of materials and structures used in impact damage protection applications. The split Hopkinson pressure bar apparatus or a drop weight testing machine is usually employed for such purposes. The measurement of impact force acting on the specimen is of course a fundamental issue in such tests.

Harrigan *et al* [48,56] conducted drop hammer tests on several materials and applied the deconvolution technique to obtain the impact force history. The specimen is placed on the upper surface of a load cell assembly (Fig. 18) and impacted with a drop hammer. The signal detected by the piezoelectric load cell does not represent the true impact force transmitted to the die due to wave propagation within the load cell assembly. The transfer function between the impact force acting on the upper surface and the signal detected by the load cell was identified by conducting a calibration test in which a long rod was used as an impactor as shown in Fig. 18. Figures 19 and 20 show typical results for testing of an American oak cylinder and a mild steel tube, respectively. In both cases, the time histories before and after deconvolution are quite different although the results are not perfect as some erroneous oscillation occurred after impact. The saw tooth pattern seen in the deconvolved force history of the mild steel tube corresponds to the formation of folds in the tube.

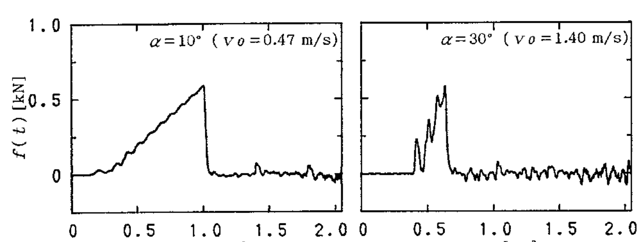

Fig. 17 Impact forces estimated by deconvolution [45].

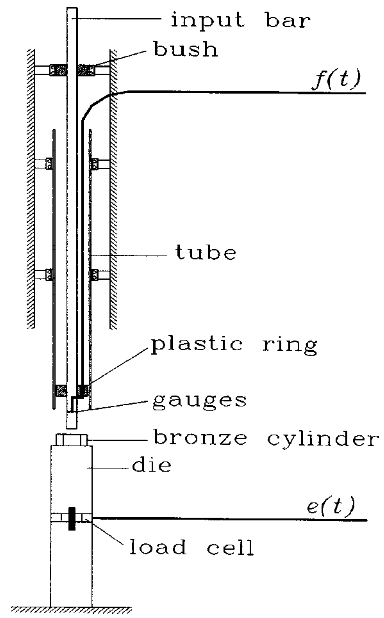

Fig. 18 The load cell assembly used in the drop-hammer dynamic-compression test [48].

3 INVERSE ANALYSIS OF DIRECTION

There are many cases in which the direction of the impact force is required to be measured in addition to the impact force history. For example, knowledge of the magnitude and direction of the impact force is helpful in understanding the mechanisms of structural damage caused by impact with foreign objects. Such measurements were difficult even in simple cases such as oblique impact of a plate with a small ball. Some techniques of inverse analysis have been developed to overcome this difficulty. In this section, it is assumed that the location of the impact force is known while both the magnitude and the direction are to be estimated.

3.1 Basic formulation

The estimation of the magnitude and direction of an impact force can be accomplished by extending the method for estimating the time history by deconvolution to the three dimensional case. If the relationship between the impact force and the response can be assumed to be linear as in the estimation of the time history, then the principle of superposition can apply. Therefore, the response at a point of the body can

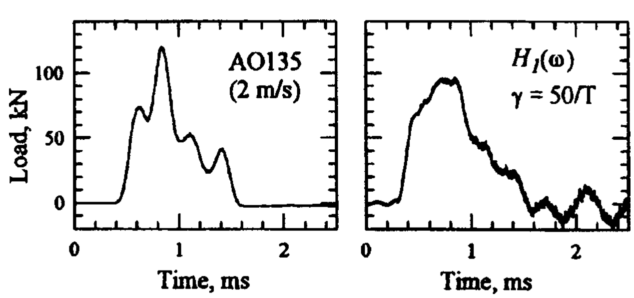

Fig. 19 Result of drop-hammer test on an American oak cylinder: before (left) and after (right) deconvolution [48].

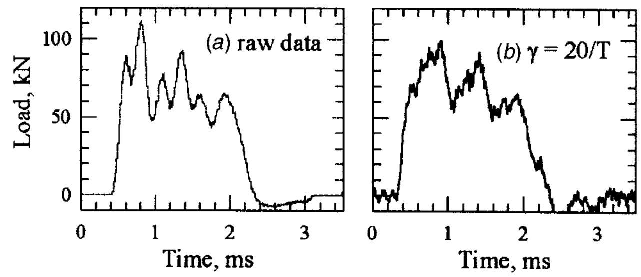

Fig. 20 Result of drop-hammer test on a mild steel tube: before *a*) and after *b*) deconvolution [48].

be expressed as a sum of responses each of which is induced by each of three components of the impact force:

$$e_j(t)=\sum_{i=1}^{3}\int_0^t h_{ji}(t-\tau)f_i(\tau)d\tau, \quad (j=1,2,\cdots), \tag{18}$$

where $f_i(t)$ is the ith component of the impact force, $e_j(t)$ is the jth component of the response and $h_{ji}(t)$ is the impulse response function between $f_i(t)$ and $e_j(t)$. The response components $e_j(t)$ $(j=1,2,\cdots)$ can be one or several components of response at a certain or several different points of the body. If all of the impulse response functions are identified in some manner and if the response components are measured, then the time histories of all components can be estimated by solving a set of integral equations (18), and hence the magnitude and direction of the impact force are derived.

3.2 Techniques of inverse analysis

Michaels and Pao [57,58] first considered this kind of problem in which an oblique impact force acting on an infinite plate was estimated from displacements normal to the plate measured at different locations of the plate. They introduced a simplification that the time histories of all components of the impact force are identical, which makes it possible to reduce Eq. (18) into a simpler form as

$$e_j(t)=\sum_{i=1}^{3} f_i\int_0^t h_{ji}(t-\tau)s(\tau)d\tau \tag{19}$$

where f_i is the magnitude of the ith component and $s(t)$ is the time variation of all components. The problem of solving Eq. (19) was separated into the following two subproblems:

1) When f_i $(i=1,2,3)$ are given, determine $s(t)$ so as to minimize the least squares error between the displacement calculated by Eq. (19) and the measured displacement. This subproblem corresponds to one-dimensional deconvolution for estimating a function $s(t)$.
2) When $s(t)$ is given, determine f_i $(i=1,2,3)$ so as to minimize the least squares error between the displacement calculated by Eq. (19) and the measured displacement. This subproblem corresponds to solving a set of algebraic equations for f_i $(i=1,2,3)$.

These two subproblems were solved alternately starting with an initial guess for f_i $(i=1,2,3)$. Final estimates of the time history $s(t)$ and direction f_i ($i=1,2,3$) of the impact force were obtained after repeating this alternate procedure. Time domain discretization of the integral in Eq. (19) was adopted for numerical solution of these two subproblems. The impulse response functions $h_{ji}(t)$ were predicted by theoretical analysis for a thick infinite plate. For this particular problem of Michaels and Pao, the direction of the impact force can be determined from displacements at only two different points with a special choice of the spatial coordinate system.

Buttle and Scruby [59,60] studied normal and oblique impacts of a plate with small particles, in which an equation the same as Eq. (18) was presented for oblique elastic impact. For oblique plastic impact, they proposed an equation

$$e_j(t)=\sum_{i=1}^{3}\int_0^t h_{ji}(t-\tau)f_i(\tau)d\tau + \sum_{i=1}^{3}\int_0^t h_{ji,i}(t-\tau)d_i(\tau)d\tau, \tag{20}$$

where $d_i(t)$ is the ith component of the force dipole induced by the plastic deformation in the vicinity of the impact site. Unfortunately, no technique to solve Eq. (20) was given. They conducted experiments only for cases of normal elastic impact in which the direction of the impact force is known in advance.

Inoue *et al* [61] proposed a general method to estimate the magnitude and direction of the impact force. They applied Fourier transformation to Eq. (18) resulting in

$$E_j(\omega)=\sum_{i=1}^{3} H_{ji}(\omega)F_i(\omega), \quad (j=1,2,\cdots), \tag{21}$$

or in matrix form

$$\begin{Bmatrix} E_1(\omega) \\ E_2(\omega) \\ \vdots \end{Bmatrix} = \begin{bmatrix} H_{11}(\omega) & H_{12}(\omega) & H_{13}(\omega) \\ H_{21}(\omega) & H_{22}(\omega) & H_{23}(\omega) \\ \vdots & \vdots & \vdots \end{bmatrix} \begin{Bmatrix} F_1(\omega) \\ F_2(\omega) \\ F_3(\omega) \end{Bmatrix}. \tag{22}$$

If the transfer functions are identified in advance, then the time histories of all components of the impact force are estimated by transforming all components of the measured responses, solving the algebraic equations (22) for $F_i(\omega)$ ($i=1,2,3$) and transforming them back into the time domain. To improve the accuracy of the estimate, both exponential windowing and the Wiener filter mentioned above can be applied. The least squares method can also be applied by setting the number of response components more than the number of force components. However, more importantly, it was pointed out that care must be taken for a combination of response components.

In principle, the combination of the response components must be arranged so that the number of mutually independent equations in the algebraic equations (22) does not become less than the number of unknowns (the number of force components). Since the number of mutually independent equations is equal to the rank of the coefficient matrix, it can be checked by computing the singular value decomposition of the coefficient matrix and counting the number of non-zero singular values. In practice, however, the algebraic equations become close to being linearly dependent, that is the coefficient matrix in Eq. (22) is ill-conditioned. If this is the case, then the solution for the force components becomes extremely sensitive to small errors involved in the response data and is likely to be highly inaccurate. The degree of ill-conditioning can be evaluated by the condition number of the coefficient matrix which is defined as the ratio of the largest singular value to the smallest non-zero singular value of the coefficient matrix. The condition number is always greater than unity. The degree of ill-conditioning becomes worse as the condition number increases. If the condition number is very large, then the combination of the response components should be rearranged by changing some of the locations and directions in which the response components are measured. A regularization technique is applicable in principle in order to relax the ill-conditioning but it does not work very well because the number of unknowns is only three.

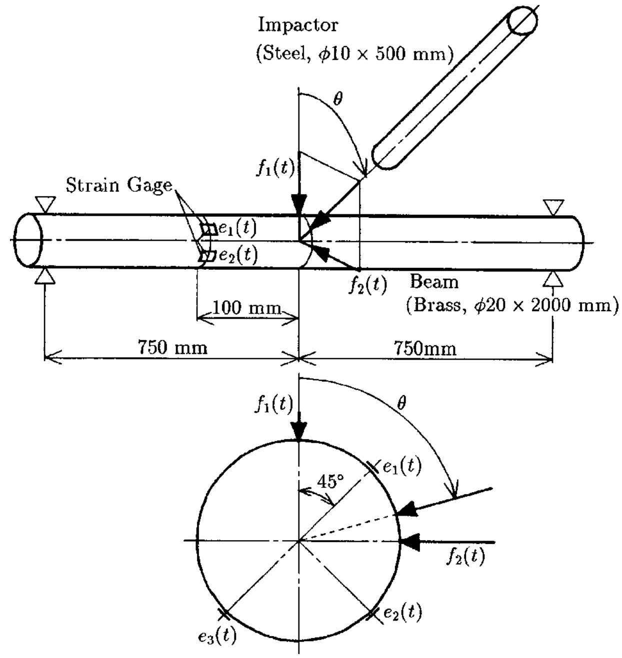

Fig. 21 A simply supported beam subjected to two-dimensional impact force at the center of its span [61].

Inoue *et al* [61] conducted an experiment to measure the magnitude and direction of a two-dimensional impact force acting on a simply supported beam as shown in Fig. 21. The transfer functions were identified experimentally by conducting calibration tests. An impact force induced by longitudinal impact of a steel rod in the direction of $\theta=75°$ was measured and compared with a direct measurement using strain gauges attached to the impactor. The estimate obtained from a good pair of strain responses (for which the condition number of the coefficient matrix is small) is in good agreement with the direct measurement (Fig. 22) while the estimate obtained from a bad pair (for which the condition number is large) is very noisy and inaccurate (Fig. 23). The reason for the difference between these two estimates is understood

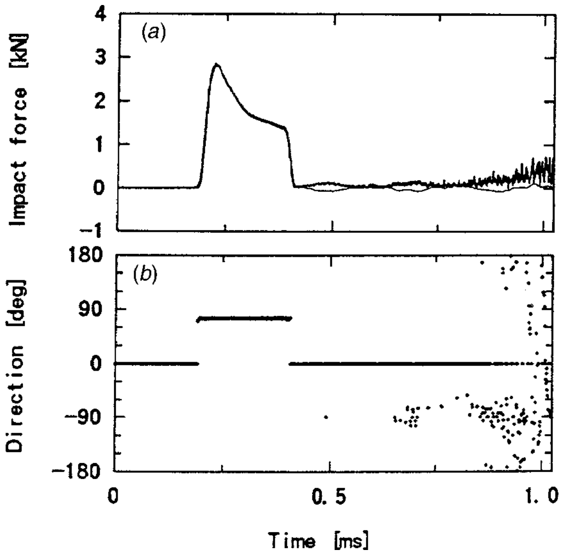

Fig. 22 The magnitude and direction of impact force estimated from a good pair of strain responses ($e_1(t)$ and $e_2(t)$) (Ref. [61]).

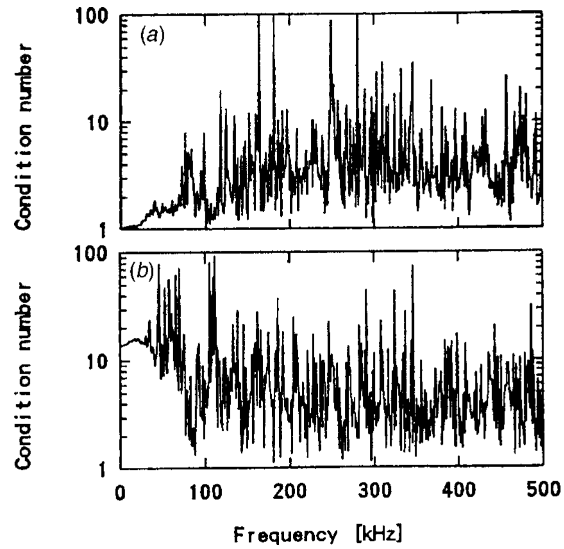

Fig. 24 The condition numbers of the transfer function matrix at every frequencies for the good pair *a*) and the bad pair *b*) of strain responses [61].

from Fig. 24 in which the condition number of the transfer function matrix is plotted against frequency for both cases. The condition number is much larger in the bad pair case (Fig. 24*b*) than in the good pair case (Fig. 24*a*) especially at lower frequencies. Although a simple regularization technique was applied to the bad pair case, the accuracy of estimation was not improved very much.

The technique to estimate the direction of an impact force can be easily extended to estimating the magnitude and direction of more than two impact forces acting simultaneously at multiple locations. Since Eq. (18) holds for each of the impact forces acting at multiple points of the body, it follows from the principle of superposition that

$$e_j(t)=\sum_{i=1}^{3N}\int_0^t h_{ji}(t-\tau)f_i(\tau)d\tau, \quad (j=1,2,\cdots), \tag{23}$$

where $f_i(t)$ $(i=1,2,\cdots,3N)$ are three components of impact forces acting at N different locations. Wu *et al* [62] studied the estimation of time histories of impact forces acting simultaneously at multiple locations of laminated plates through numerical simulation and experiment. They conducted an experiment in which a freely-supported graphite-epoxy-laminated plate was subjected to impact forces at three locations and the strain responses were measured at three locations as shown in Fig. 25. The deconvolution technique employed was the same as in their previous papers [8,10]. Since the directions of impact forces were known in this experiment, only the time histories of three impact

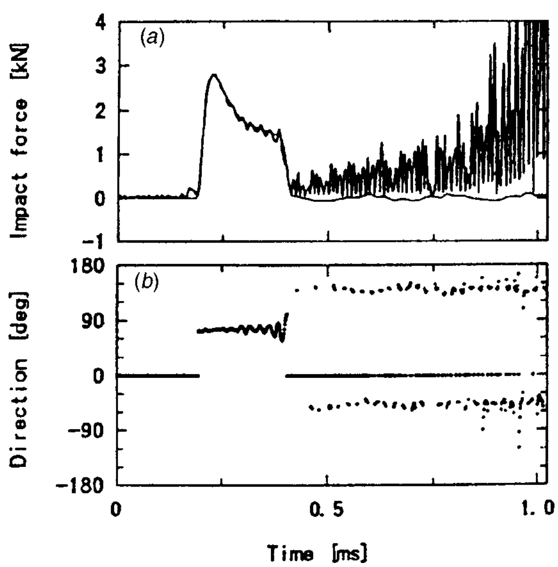

Fig. 23 The magnitude and direction of impact force estimated from a bad pair of strain responses ($e_1(t)$ and $e_3(t)$) (Ref. [61]).

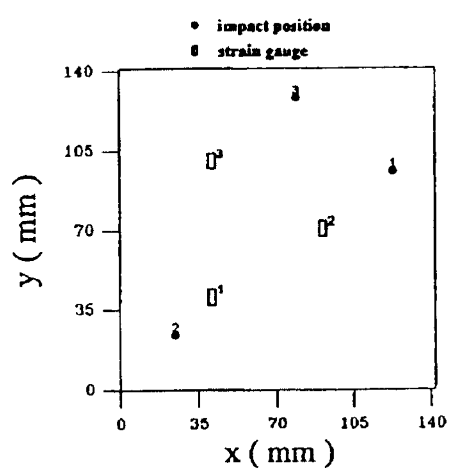

Fig. 25 Locations of impact and strain gauges of a laminated plate [62]. (Reprinted with permission from the American Institute of Aeronautics and Astronautics.)

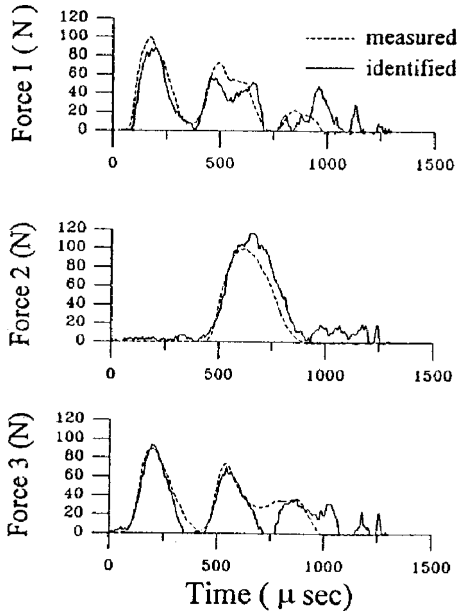

Fig. 26 Three impact forces estimated from strain responses and measured by impact hammers [62]. (Reprinted with permission from the American Institute of Aeronautics and Astronautics.)

forces were estimated. The resultant estimates agree well with measurements obtained by impact hammers as shown in Fig. 26.

4 INVERSE ANALYSIS OF LOCATION

The location of an impact force may be required in the on-line monitoring of structures subjected to impact because there is a risk of fatal injuries or serious damages for which quick measures should be taken. If further knowledge is required, then some of the techniques mentioned so far could be applied later to estimating the time history or the direction of the impact force. Therefore, estimating the location is considered as the first step to a full understanding of the impact force.

The inverse problem to estimate the location of the impact force is basically a nonlinear problem even for elastic structures, and hence there are much greater difficulties in solving it compared with inverse problems of estimating the time history or the direction of the impact force. In principle, the location is estimated from the velocities of stress waves and their arrival times at several points of the structure. However, determination of wave velocities is not an easy task for real structures having complex shapes and, in addition, detection of arrival times is also difficult in practice because of reflections, refractions and dispersions of stress waves. For this reason, very few techniques have been developed which can be applied generally to real structures. Most of the techniques developed so far are applicable only to beams or plates.

A variety of techniques have been developed for detecting the location of transient disturbances such as earthquake sources, acoustic emission sources and noisy sound sources. Many of them may be also applicable to estimating the location of an impact force, but will not be presented here. Instead, attention will be paid to those which directly deal with impact on structures.

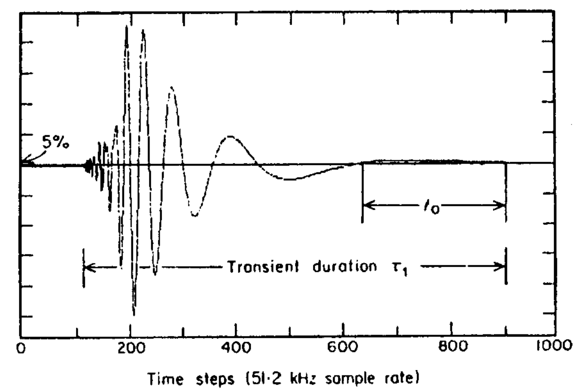

Fig. 27 Acceleration response at a location away from the impact location for Hertzian impact of an infinite beam [35]. (Reprinted with permission from the Academic Press.)

4.1 Impact location of beams and frames

Whiston [35] and Jordan and Whiston [36] developed a technique for estimating the impact location on infinite beams. This technique is composed of two stages based on Timoshenko beam theory. It is assumed that the impact force is impulsive, like a half-sine pulse of very short duration. The first stage provides a relatively rough estimate. If a response to an impulsive force is recorded at a point away from the impact location, then it has a duration, say τ_1 as shown in Fig. 27, which is caused by wave dispersion. According to Timoshenko theory, the fastest wave component in the response has a velocity close to the shear wave velocity c_s in an elastic medium. On the other hand, a slowest *significant* component has a velocity $c(\omega_0)$ at a frequency $\omega_0=\pi/t_0$, where t_0 can be roughly estimated as shown in Fig. 27. From the difference in the arrival times of these two wave components, the distance from the impact location to the measuring point can be estimated as

$$x=\tau_1 c_s c(\omega_0)/[c_s-c(\omega_0)]. \tag{24}$$

Since the above equation provides only the distance from the impact location, two measurements at different points are required to determine the impact location uniquely. The second stage is linked with the estimation of the impact force history by means of deconvolution using the transfer function predicted by Timoshenko theory. If the distance is underestimated, then the estimate of the time history shows an initial negative spike (Fig. 28*a*). If the distance is overestimated, on the other hand, it has a final negative spike (Fig. 28*c*). Therefore, the estimate obtained in the first stage is refined if correction is made so that the estimate of the time history does not have a negative spike (Fig. 28*b*). The main restriction on applying this technique in practice is that the impact force must be impulsive (which cannot be verified in advance). In addition, a considerable amount of human interference is required for determining both the frequency of the

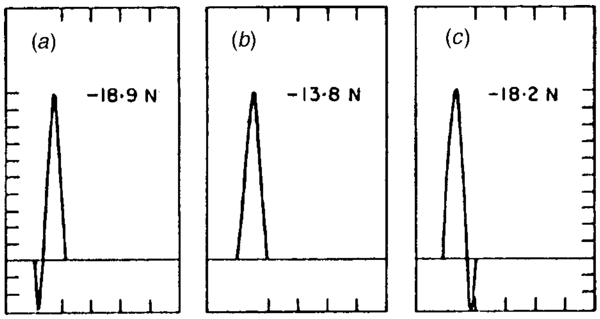

Fig. 28 The effect of small errors in distance on the estimate of the time history by deconvolution: *a*) underestimation of distance, *b*) correct estimation of distance and *c*) overestimation of distance [35]. (Reprinted with permission from the Academic Press.)

slowest *significant* component, ω_0, from a response record and removing the negative spike from the estimate of the time history.

Doyle [63] also considered estimation of the impact location for beams, in which phase information is utilized. Based on Bernoulli-Euler beam theory, the relationship between the distance from the impact location x and the phase of the measured response $\phi(x,\omega)$ is expressed as

$$\phi(x,\omega)=\phi(0,\omega)+\theta(x,\omega)-k(\omega)x, \tag{25}$$

where $\theta(\omega)$ is the contribution of the ringing term involved in Bernoulli-Euler theory and $k(\omega)$ is the wave number. If measurements are made at two points, say x_1 and x_2, and if the impact location lies between them $(x_1+x_2=L)$, then the distance x_1 can be expressed as

$$x_1=L-\frac{d}{dk}[\phi(x_1,\omega)-\phi(x_2,\omega)-\theta(x_1,\omega)+\theta(x_2,\omega)]. \tag{26}$$

In this equation, $\phi(x_1,\omega)$ and $\phi(x_2,\omega)$ are obtained from Fourier transforms of the measured responses. Although $\theta(x_1,\omega)$ and $\theta(x_2,\omega)$ are originally unknown, they can be computed if x_1 and x_2 are given. Therefore, Eq. (26) can be solved for x_1 in an iterative manner beginning with an appropriate guess for x_1. The estimate of the distance is independently obtained at each frequency, which means that a more reliable estimate can be deduced from estimates at all frequencies considered. The main disadvantage of this technique is that it requires an appropriate guess of the distance x_1 before the estimate can be refined.

Choi and Chang [64] studied simultaneous estimation of the location and the impact force history on a beam from responses obtained by several sensors distributed on the beam. They employed a state variable formulation based on Bernoulli-Euler theory and considered minimization of an objective function in terms of the location and the time history. Unfortunately, only the outline of the technique was presented in their paper. In addition, the proposed objective function is correct in principle but involves too many variables to be optimized, which might cause difficulties in the optimization process.

Most of the shortcomings of the three techniques mentioned above may be overcome by a technique developed by

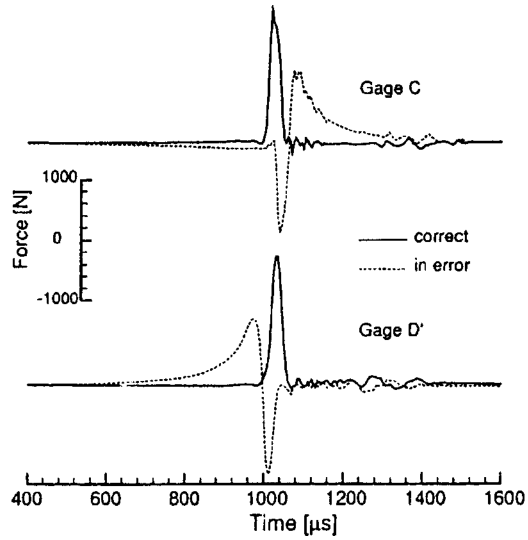

Fig. 29 Effect of error in the guess of the impact location on the estimates of the time history [65]. (Reprinted with permission from the Society for Experimental Mechanics.)

Doyle [65]. This technique is linked with the estimation of the time history of an impact force based on Timoshenko beam theory. Impact responses of the beam are measured at two points straddling the impact location. With an initial guess of the impact location, two independent estimates of the time history are obtained from these two responses by deconvolution in which the transfer function is predicted as a function of the guessed impact location by Timoshenko theory. These two estimates coincide well if the guess of the impact location is correct while they differ from each other if the guess is in error (Fig. 29). To quantify the degree of coincidence, Doyle utilized the correlation between these two estimates

$$C_{12}=\sum_k f_1(k\Delta t)f_2(k\Delta t), \tag{27}$$

where $f_1(k\Delta t)$ and $f_2(k\Delta t)$ are two estimates of the time history in discrete form. An example of the correlation is shown in Fig. 30 as a function of guessed impact location. A correct estimate of the location is obtained by maximizing the correlation. Since the correlation has many local maxima, he employed a genetic algorithm to search for a global maximum of the correlation. A genetic algorithm is a stochastic search technique modeled on the natural process of evolution. An example of convergence of this algorithm is demonstrated in Fig. 31, in which a correct estimate of the location is obtained after 10 generations. This technique of using a genetic algorithm was further extended by Martin and Doyle [66] to be applicable to frame structures. First, an efficient method was developed for predicting the transfer function as a function of guessed impact location because a number of deconvolutions are required in the search process. Secondly, instead of the correlation mentioned above, they proposed another objective function based on the differences between two estimates of the impact force. It should be noted

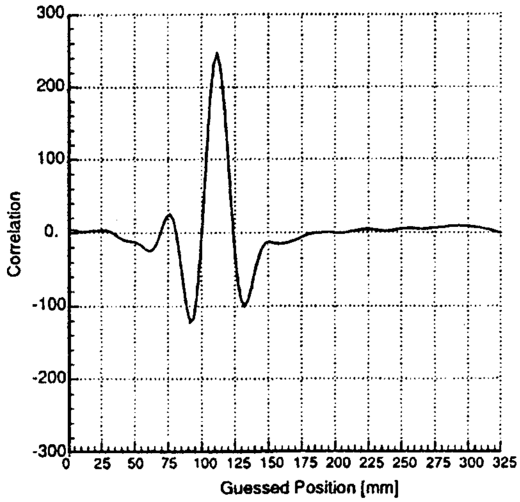

Fig. 30 Correlation between two estimates of the time history as a function of guessed impact location [65]. (Reprinted with permission from the Society for Experimental Mechanics.)

that in a genetic algorithm an appropriate tuning of parameters is essential for attaining a sufficiently fast convergence of the searching process.

A technique which does not rely on beam theory was proposed by Inoue *et al* [67]. In their preceding paper (Kishimoto *et al* [68]), it was shown that when a pulse propagating in a dispersive medium is recorded at a point, the arrival time of each frequency component of the pulse at that point can be detected by a time-frequency analysis by means of wavelet transform. They utilized this fact to estimate the wave velocity and the impact location for beams. The impact responses of a beam are measured at two points lying on one side of the impact location (P_1 and P_2) and at a point on the other side (P_3) as shown in Fig. 32. The arrival time of each frequency component is related to the distance from the impact location l_k by

$$b_k(\omega)=b_0(\omega)+l_k/c_g(\omega), \quad (k=1,2,3), \tag{28}$$

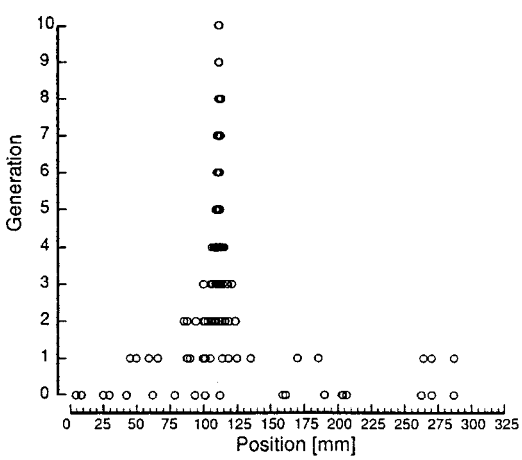

Fig. 31 Convergence of population over the generations [65]. (Reprinted with permission from the Society for Experimental Mechanics.)

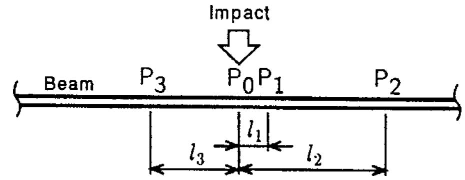

Fig. 32 Arrangement of sensors for estimating the wave velocity and the impact location [67]. (Reprinted with permission from the Society for Experimental Mechanics.)

where $b_k(\omega)$ is the arrival time at point P_k, $b_0(\omega)$ is an unknown time lag associated with the wavelet transform and $c_g(\omega)$ is the group velocity of the flexural waves in the beam. The following equations are derived from Eq. (28):

$$c_g(\omega)=\frac{l_2-l_1}{b_2(\omega)-b_1(\omega)} \tag{29}$$

and

$$b_0(\omega)=\frac{1}{2}\left[b_1(\omega)+b_3(\omega)-\frac{l_1+l_3}{c_g(\omega)}\right]. \tag{30}$$

Since the distances (l_2-l_1) and (l_1+l_3) are known in advance and, in addition, the arrival times $b_k(\omega)$ $(k=1,2,3)$ are detected by time-frequency analyses of measured responses, $c_g(\omega)$ is obtained by Eq. (29) and then $b_0(\omega)$ is obtained by Eq. (30). Once $c_g(\omega)$ and $b_0(\omega)$ are obtained, the distances l_k $(k=1,2,3)$ are easily estimated by Eq. (28). An experiment was conducted on a simply supported beam with a circular cross section subjected to impact with a steel ball. Both the group velocity and the impact location were estimated successfully as shown in Fig. 33. The scatter at higher frequencies is caused by the poor signal-to-noise ratio of the experimental data. The main advantage of this technique is that the estimate of the impact location is obtained

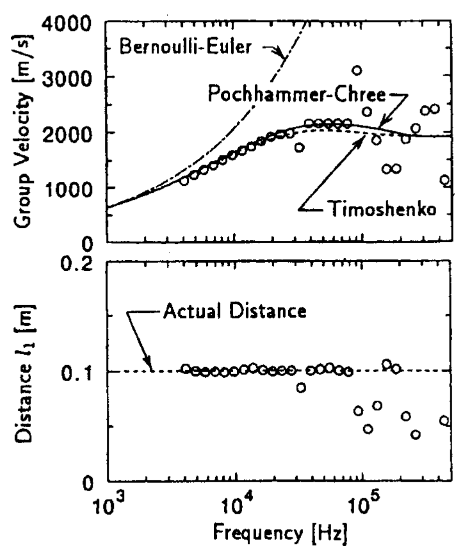

Fig. 33 The group velocity and impact location estimated by a time-frequency analysis by means of wavelet transform [67]. (Reprinted with permission from the Society for Experimental Mechanics.)

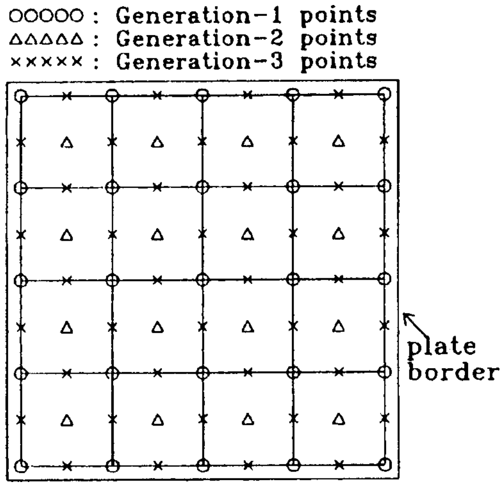

Fig. 34 Schematic of the procedure for grid point generation [44].

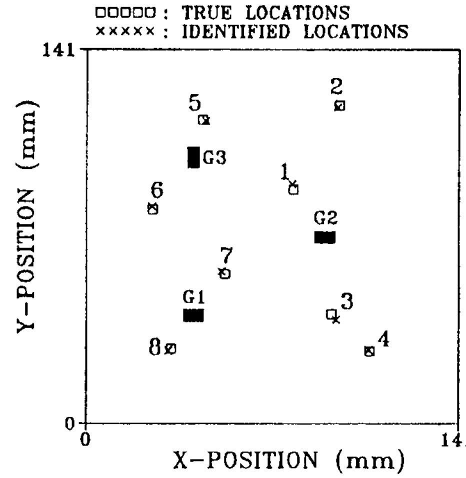

Fig. 35 Comparisons of the identified and the true impact locations for the eight examples using a hammer as the impactor. Arrangement of the strain gages (G1, G2, G3) is also shown [9].

only from experimental records without using beam theory. Therefore, this technique can be extended to be applicable to other structures more easily than other techniques.

4.2 Impact location for plates

The earliest study on the inverse analysis of the impact location for plates is probably the one by Yen and Wu [9,44]. They developed a technique for estimating the impact location for plates subjected to transverse impact from strain responses measured at multiple points on the plate. For a pair of points, they derived the following mutuality relationship from Eq. (2):

$$\boldsymbol{h}_i\boldsymbol{e}_j=\boldsymbol{h}_j\boldsymbol{e}_i, \tag{31}$$

where the subscript stands for the measuring point. The vectors $\boldsymbol{e}_i$ and $\boldsymbol{e}_j$ are composed of discrete values of measured responses while the matrices $\boldsymbol{h}_i$ and $\boldsymbol{h}_j$ are composed of discrete values of the impulse response functions which are expressed in terms of the impact location according to Reissner-Mindlin plate theory. Equation (31) is satisfied if $\boldsymbol{h}_i$ and $\boldsymbol{h}_j$ are evaluated using the correct impact location. Based on this fact, estimation of the unknown impact location was reduced to an optimization problem minimizing

$$\sum_{i=1}^{N}\sum_{j=1,j\neq i}^{N}\frac{\|\boldsymbol{h}_i\boldsymbol{e}_j-\boldsymbol{h}_j\boldsymbol{e}_i\|^2}{\|\boldsymbol{h}_i\boldsymbol{e}_j\|^2}, \tag{32}$$

where N is the total number of measuring points and the denominator $\|\boldsymbol{h}_i\boldsymbol{e}_j\|^2$ is introduced to avoid meaningless solutions. Since this objective function has many local minima, they employed a strategy shown schematically in Fig. 34. The objective function is first evaluated at all grid points denoted by Generation-1. Then an optimization process based on the conjugate gradient method is performed starting from a grid point which has the smallest value of the objective function among all of the grid points. If the value of the objective function at the point obtained by the optimization process is smaller than a prescribed value, this point is considered as the impact location. Otherwise, the same procedure is repeated for grid points of the next generation. The validity of this technique was demonstrated by numerical simulations [44], as well as by experiments [9]. Figure 35 shows typical results of experiments. Every estimate coincides well with the true impact locations. The convergence of the optimization process seems good.

Ohkami and Tanaka [69] proposed a two-stage technique based on classical plate theory. The first stage is to determine an elliptic region which may contain the true impact location. The impact responses of a plate are measured at more than three points. For a pair of points, say P_1 and P_2, the difference Δt_{12} between first arrival times of the pulse originating from the impact location is roughly evaluated to be equal to the time lag at which the cross-correlation function between responses at these two points becomes maximum. Then for a set of three points, say P_1, P_2 and P_3, a rough estimate of the impact location (x,y) is obtained from the time differences Δt_{12} and Δt_{13} and from the fastest phase velocity predicted by plate theory. In the same manner, similar estimates of the impact location are obtained for different sets of three points. Taking the means (m_x and m_y) and the standard deviations (σ_x and σ_y) of these estimates, an elliptic region is determined by setting the center at (m_x,m_y) and the semi-axes at $2\sigma_x$ and $2\sigma_y$. An example is shown in Fig. 36 in which four estimates of the impact location are obtained from responses measured at four points. The second stage is linked with the estimation of the impact force history. The elliptic region is divided into meshes each of which is a candidate for the true impact location. Assuming that one of these mesh points is the impact location, the impact force history is estimated by deconvolution from the response measured at some point and the transfer function predicted by plate theory. Similar estimates of the time history are thus obtained for all mesh points. Based on evaluation of a penalty quadratic form of the estimated time history (it has a similar form as Eq. (5) but the parameter λ is fixed at an appropriate value), one of these mesh point is selected as a final estimate of the impact location. An example of evaluation of the penalty quadratic form is shown in Fig. 37 in

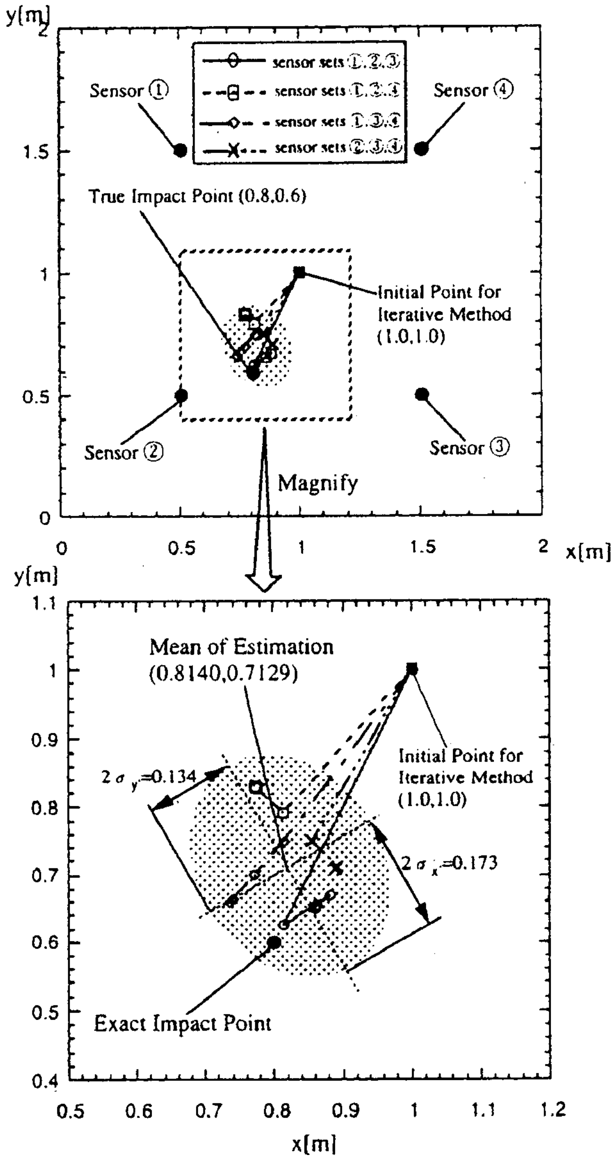

Fig. 36 Determination of an elliptic region containing the impact location [69]. (Reprinted with permission from the Japan Society for Mechanical Engineers.)

which a mesh point at which the penalty quadratic form becomes maximum (point (i)) coincides with the true impact location. Although it has not been described here in detail, even in the simple numerical simulation shown in the paper by Ohkami and Tanaka, frequent human interferences are required both in determining the elliptic region and in selecting a final estimate of the impact location from candidates.

Gaul and Hurlebaus [70] extended the technique mentioned above for identifying the impact location of beams by using wavelets [67] to the identification of the impact location of plates. The impact location is estimated by solving a simple system of nonlinear equations based on arrival times of flexural waves at several points of a plate. Since the arrival times can be extracted accurately by using the wavelet transform, the process of estimation of the impact location is much simpler than that by Ohkami and Tanaka [69]. The result of the estimation shown in this paper seems very accurate. Since this technique does not rely on plate theory, it should be possible to extend this technique to anisotropic plates such as composites.

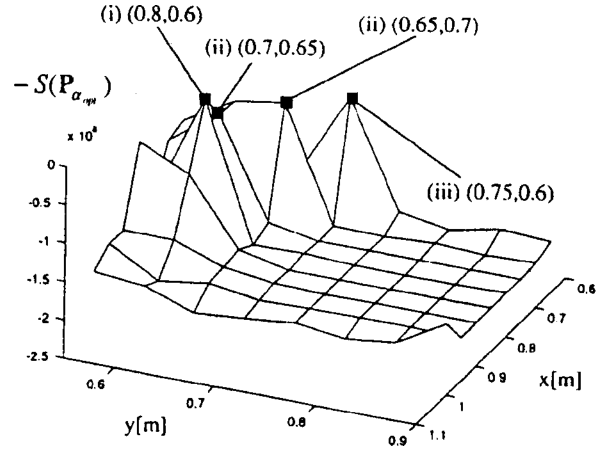

Fig. 37 Distribution of the penalty quadratic form of the estimated time history [69]. (Reprinted with permission from the Japan Society for Mechanical Engineers.)

4.3 Impact location for other structures

There are very few studies on techniques for estimating the impact location for an arbitrary structure. Briggs and Tse [71] proposed a technique based on modal analysis and pattern matching. First, the transfer function between an impact force and a response is modeled as a summation of different modes:

$$\frac{E_j(\omega)}{F_k(\omega)} = -\omega^2 \sum_{r=1}^{n} \frac{A_{rjk}}{\omega_r^2 - \omega^2 + i\,\eta_r \omega_r^2}, \tag{33}$$

where $E_j(\omega)$ and $F_k(\omega)$ are the Fourier transforms of the response at location j and the impact force at location k, respectively. In addition, ω_r and η_r are the natural frequency and the loss factor of the rth mode, respectively, and A_{rjk} is the modal constant. If the impact force is a pulse of short duration, $F_k(\omega)$ has fairly constant magnitude for lower frequencies. When this is the case, Eq. (33) can be rewritten as

$$E_j(\omega) = -\omega^2 \sum_{r=1}^{n} \frac{A^*_{rjk}}{\omega_r^2 - \omega^2 + i\,\eta_r \omega_r^2}, \tag{34}$$

where $A^*_{rjk} \equiv F_k(\omega) A_{rjk}$. Note that A^*_{rjk} (which is termed the uncorrected modal constant) does not depend on the frequency. All parameters A^*_{rjk}, ω_r, and η_r are determined in advance for each location k on the structure where impact is likely to occur. This is accomplished by applying an impact force of short duration to each location k, measuring the response at location j, and conducting a standard modal parameter extraction procedure (curve fitting). Thus a database of the uncorrected modal constants is constructed for all possible impact locations. When an impact occurs at an unknown location on the structure, the recorded response signal is transformed into the frequency domain and curve-fitted to extract the uncorrected modal constants. The extracted modal constants are compared with those in the database. Then an

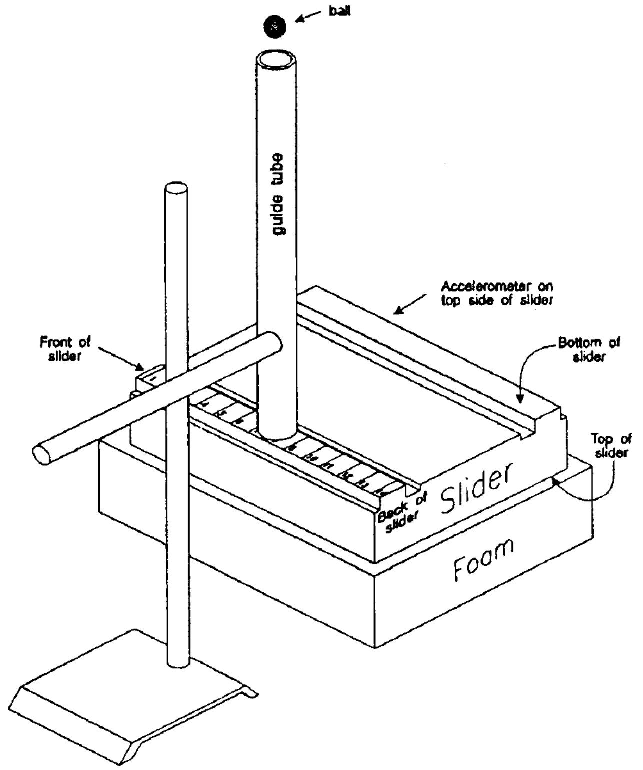

Fig. 38 Schematic of ball drop test apparatus and test structure used for testing the force identification technique [71]. (Reprinted with permission from Elsevier Science.)

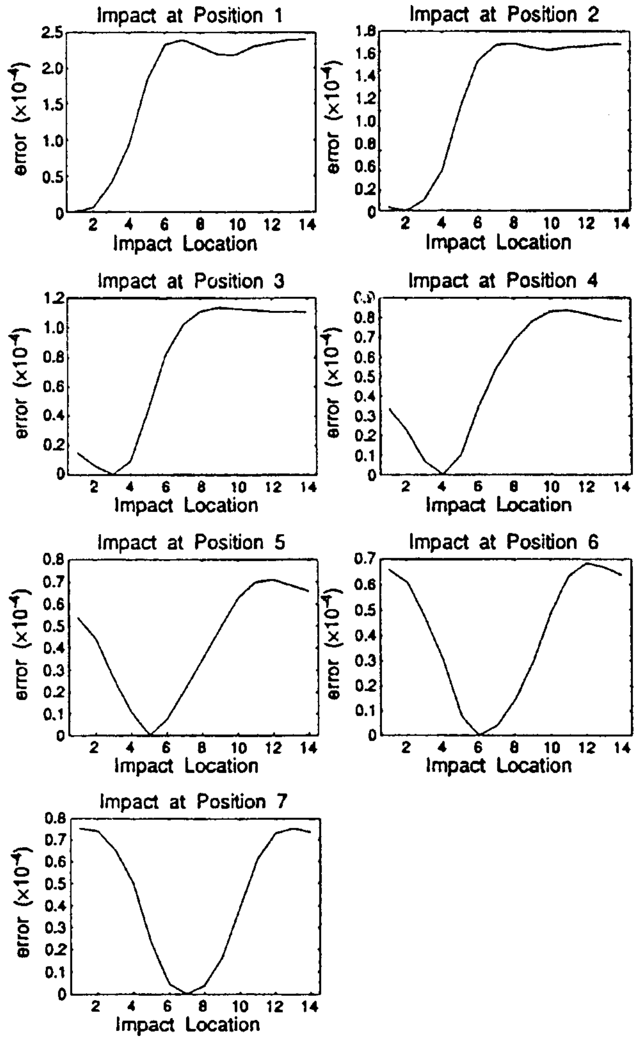

Fig. 39 Error plots resulting from pattern matching between the uncorrected modal constants and the database of modal constants using the magnitude and phase information in the acceleration signal [71]. (Reprinted with permission from Elsevier Science.)

estimate of the impact location is obtained by a pattern matching scheme. Briggs and Tse conducted an experiment on impact of an enlarged model of a slider used in magnetic hard disk drives as shown in Fig. 38. After constructing a database of the modal constants for the first four modes, the location of impact was estimated as shown in Fig. 39. The error resulting from pattern matching becomes minimum at the true impact location for all cases shown, which demonstrates the validity of this technique. The main disadvantage of this technique is that it requires a huge amount of work to construct a database of the uncorrected modal constants. However, once the database is constructed appropriately, the procedure to estimate the impact location seems fairly simple and easy to implement in practice.

5 CONCLUSIONS

The aquisition and measurement of accurate force pulse data is of central importance in many modern branches of impact mechanics. A variety of approaches for measuring the time history, direction and location of such pulses have been described and the related data processing techniques discussed. Workers in the field have drawn heavily on procedures in control theory, optimization, stochastic search techniques (genetic algorithm), and other areas to good effect. With the advent of accurate transducers, accurate data recording equipment and efficient data processing software, the methods reviewed should be of assistance in enabling researchers to produce reliable and detailed information on impact forces which will assist in the validation of theoretical models for structural response and in the understanding of material behavior under impact and impulsive loading conditions.

A Supplemental Bibliography of additional references that the authors noticed during the review process of this paper are listed at the end.

REFERENCES

[1] Lundberg B and Henchoz A (1977), Analysis of elastic waves from two-point strain measurement, *Exp. Mech.* **17**, 213–218.
[2] Engl HW, Hanke M, and Neubauer A (1996), *Regularization of Inverse Problems*, Kluwer Academic, Dordrecht.
[3] Groetsch CW (1993), *Inverse Problems in the Mathematical Sciences*, Vieweg, Braunschweig.
[4] Stevens KK (1987), Force identification problems—an overview, *Proc 1987 SEM Spring Conf Exp Mech, Houston*, SEM, 838–844.
[5] Goodier JN, Jahsman WE, and Ripperger EA (1959), An experimental surface-wave method for recording force-time curves in elastic impacts, *ASME J. Appl. Mech.* **26**, 3–7.
[6] Doyle JF (1984), An experimental method for determining the dynamic contact law, *Exp. Mech.* **24**, 10–16.
[7] Chang C and Sun CT (1989), Determining transverse impact force on a composite laminate by signal deconvolution, *Exp. Mech.* **29**, 414–419.
[8] Wu E, Tsai T-D, and Yen C-S (1995), Two methods for determining

impact-force history on elastic plates, *Exp. Mech.* **35**, 11–18.

[9] Yen C-S and Wu E (1995), On the inverse problem of rectangular plates subjected to elastic impact, Part II: Experimental verification and further applications, *ASME J. Appl. Mech.* **62**, 699–705.

[10] Wu E, Yeh J-C, and Yen C-S (1994), Impact on composite laminated plates: an inverse method, *Int. J. Impact Eng.* **15**, 417–433.

[11] Tsai C-Z, Wu E, and Luo B-H (1998), Forward and inverse analysis for impact on sandwich panels, *AIAA J.* **36**, 2130–2136.

[12] Hansen PC (1998), *Rank-Deficient and Discrete Ill-Posed Problems*, SIAM, Philadelphia.

[13] Tanaka H and Ohkami Y (1997), Estimation of impact force on a space vehicle based on an inverse analysis technique (in Japanese), *Trans. Jpn. Soc. Mech. Eng., Ser. C* **63C**, 1172–1178.

[14] Hojo A, Chatani A, and Uemura F (1989), An estimation of impact force by convolution integral (in Japanese), *Trans. Jpn. Soc. Mech. Eng., Ser. A* **55A**, 477–482.

[15] Zhu J and Lu Z (1991), A time domain method for identifying dynamic loads on continuous systems, *J. Sound Vib.* **148**, 137–146.

[16] Holzer AJ (1978), A technique for obtaining compressive strength at high strain rates using short load cells, *Int. J. Mech. Sci.* **20**, 553–560.

[17] Doyle JF (1984), Further developments in determining the dynamic contact law, *Exp. Mech.* **24**, 265–270.

[18] Doyle JF (1987), Determining the contact force during the transverse impact of plates, *Exp. Mech.* **27**, 68–72.

[19] Doyle JF (1987), Experimentally determining the contact force during the transverse impact of an orthotropic plate, *J. Sound Vib.* **118**, 441–448.

[20] Doyle JF (1993), Force identification from dynamic responses of a bimaterial beam, *Exp. Mech.* **33**, 64–69.

[21] Martin MT and Doyle JF (1996), Impact force identification from wave propagation responses, *Int. J. Impact Eng.* **18**, 65–77.

[22] Rizzi SA and Doyle JF (1989), Force identification for impact problems on a half plane, *Computational Techniques for Contact, Impact, Penetration, and Perforation of Solids*, ASME AMD-103, 163–182.

[23] Inoue H, Watanabe R, Shibuya T, and Koizumi T (1989), Measurement of impact force by the deconvolution method, *Trans JSNDI* **2**, 63–73.

[24] Inoue H, Shibuya T, Koizumi T, and Fukuchi J (1989), Measurement of impact force applied to a plate by the deconvolution method, *Trans JSNDI* **2**, 74–83.

[25] Wilcox DJ (1978), Numerical Laplace transformation and inversion, *Int. J. Electr. Eng. Educ.* **15**, 247–265.

[26] Inoue H, Kamibayashi M, Kishimoto K, Shibuya T, and Koizumi T (1992), Numerical Laplace transformation and inversion using fast Fourier transform, *JSME Int. J., Ser. I* **35I**, 319–324.

[27] Nakao T, Tanaka C, and Takahashi A (1988), Source wave analysis of impact force on wood based panel floor (in Japanese), *J. Soc. Mater. Sci. Jpn.* **37**, 565–570.

[28] Inoue H, Kishimoto K, Shibuya T, and Harada K (1998), Regularization of numerical inversion of the Laplace transform for the inverse analysis of impact force, *JSME Int. J., Ser. A* **41A**, 473–480.

[29] Hansen PC (1992), Analysis of discrete ill-posed problems by means of the L-curve, *SIAM Rev.* **34**, 561–580.

[30] Inoue H, Kishimoto K, Shibuya T, and Koizumi T (1993), Estimation of impact force by an inverse analysis, *Inverse Problems in Engineering Mechanics (IUTAM Symp, Tokyo, Japan)*, Springer-Verlag, 169–178.

[31] Inoue H, Kishimoto K, Shibuya T, and Koizumi T (1992), Estimation of impact load by inverse analysis (Optimal transfer function for inverse analysis), *JSME Int. J., SER. I* **35I**, 420–427.

[32] Kishimoto K, Inoue H, Shibuya T, and Koizumi T (1993), An inverse analysis of impact load (Measurement of impact force of cantilever by applying the optimal transfer function), *Computational Engineering (1st Pan-Pacific Conf Comput Eng, Seoul, Korea)*, Elsevier, 309–314.

[33] Bertero M, De Mol C, and Viano GA (1980), The stability of inverse problems, *Inverse Scattering Problems in Optics*, Springer-Verlag, 161–214.

[34] Doyle JF (1997), A wavelet deconvolution method for impact force identification, *Exp. Mech.* **37**, 403–408.

[35] Whiston GS (1984), Remote impact analysis by use of propagated acceleration signals, I: Theoretical methods, *J. Sound Vib.* **97**, 35–51.

[36] Jordan RW and Whiston GS (1984), Remote impact analysis by use of propagated acceleration signals, II: Comparison between theory and experiment, *J. Sound Vib.* **97**, 53–63.

[37] Kishimoto K, Kuroda M, Aoki S, and Sakata M (1986), A measuring system for dynamic stress intensity factors using a FFT analyzer (in Japanese), *J. Soc. Mater. Sci. Jpn.* **35**, 850–853.

[38] Inoue H, Shibuya T, Koizumi T, and Kishimoto K (1990), Measurement of impact load in instrumented impact testing (in Japanese), *J JSNDI* **39**, 390–395.

[39] Bateman VI, Carne TG, Gregory DL, Attaway SW, and Yoshimura HR (1991), Force reconstruction for impact tests, *ASME J. Vibr. Acoust.* **113**, 192–200.

[40] Kim JT and Lyon RH (1992), Cepstral analysis as a tool for robust processing, deverbaration and detection of transients, *Mech. Syst. Signal Process.* **6**, 1–15.

[41] Lin SQ and Bapat CN (1993), Extension of clearance and impact force estimation approaches to a beam-stop system, *J. Sound Vib.* **163**, 423–428.

[42] McCarthy DJ and Lyon RH (1995), Recovery of impact signatures in machine structures, *Mech. Syst. Signal Process.* **9**, 465–483.

[43] Daubechies I (1992), Ten lectures on wavelets, SIAM, Philadelphia.

[44] Yen C-S and Wu E (1995), On the inverse problem of rectangular plates subjected to elastic impact, Part I: Method development and numerical verification, *ASME J. Appl. Mech.* **62**, 692–698.

[45] Inoue H, Ishida H, Kishimoto K, and Shibuya T (1991), Measurement of impact load by using an inverse analysis technique (Comparison of methods for estimating the transfer function and its application to the instrumented Charpy impact test), *JSME Int. J., Ser. I* **34I**, 453–458.

[46] Tohyama M and Lyon RH (1989), Transfer function phase and truncated impulse response, *J. Acoust. Soc. Am.* **86**, 2025–2029.

[47] Wu E, Tsai C-Z, and Tseng L-H (1998), A deconvolution method for force reconstruction in rods under axial impact, *J. Acoust. Soc. Am.* **104 Pt 1**, 1418–1426.

[48] Harrigan JJ, Reid SR, and Reddy TY (1998), Accurate measurement of impact force pulses in deforming structural components, *Experimental Mechanics, Advances in Design, Testing and Analysis*, (*Proc 11th Int Conf Exp Mech, Oxford, UK*), Balkema, 149–154.

[49] DeRusso PM, Roy RJ, Close CM, and Desrochers AA (1998), *State Variables for Engineers,* 2nd ed, John Wiley & Sons, New York.

[50] Trujillo DM and Busby HR (1997), *Practical Inverse Analysis on Engineering*, CRC Press.

[51] Hollandsworth PE and Busby HR (1989), Impact force identification using the general inverse technique, *Int J. Impact Eng.* **8**, 315–322.

[52] Busby HR and Trujillo DM (1993), An inverse problem for a plate under pulse loading, *Inverse Problems in Engineering: Theory and Practice (1st Conference in a Series on Inverse Problems in Engineering, Palm Coast, FL)*, ASME, 155–161.

[53] Bateman VI, Carne TG, and McCall DM (1992), Force reconstruction for impact tests of an energy-absorbing nose, *Int. J. Anal. Exp. Modal Anal.* **7**, 41–50.

[54] Chandrashekhara K, Chukwujekwu Okafor A, and Jiang YP (1998), Estimation of contact force on composite plates using impact-induced strain and neural networks, *Composites, Part B* **29B**, 363–370.

[55] Kishimoto K, Inoue H, and Shibuya T (2000), Dynamic force calibration for measuring impact fracture toughness using the Charpy testing machine, *Pendulum Impact Testing: A Century of Progress*, ASTM STP **1380**, 253–266.

[56] Harrigan JJ, Reid SR, and Reddy TY (1998), Inertial effects on the crushing strength of wood loaded along the grain, *Experimental Mechanics, Advances in Design, Testing and Analysis, (Proc 11th Int Conf Exp Mech, Oxford, UK)*, Balkema, 193–198.

[57] Michaels JE and Pao Y-H (1985), The inverse source problem for an oblique force on an elastic plate, *J. Acoust. Soc. Am.* **77**, 2005–2011.

[58] Michaels JE and Pao Y-H (1986), Determination of dynamic forces from wave motion measurements, *ASME J. Appl. Mech.* **53**, 61–68.

[59] Buttle DJ and Scruby CB (1990), Characterization of particle impact by quantitative acoustic emission, *Wear* **137**, 63–90.

[60] Buttle DJ and Scruby CB (1991), Characterization of dust impact process at low velocity by acoustic emission, *Acoustic Emission: Current Practice and Future Directions*, ASTM STP **1077**, 273–286.

[61] Inoue H, Ikeda N, Kishimoto K, Shibuya T, and Koizumi T (1995), Inverse analysis of the magnitude and direction of impact force, *JSME Int. J., Ser. A* **38A**, 84–91.

[62] Wu E, Yeh J-C, and Yen C-S (1994), Identification of impact forces at multiple locations on laminated plates, *AIAA J.* **32**, 2433–2439.

[63] Doyle JF (1987), An experimental method for determining the location and time of initiation of an unknown dispersing pulse, *Exp. Mech.* **27**, 229–233.

[64] Choi K and Chang F-K (1994), Identification of foreign object impact in structures using distributed sensors, *J. Intell. Mater. Syst. Struct.* **5**, 864–869.

[65] Doyle JF (1994), A genetic algorithm for determining the location of structural impacts, *Exp. Mech.* **34**, 37–44.

[66] Martin MT and Doyle JF (1996), Impact force location in frame structures, *Int. J. Impact Eng.* **18**, 79–97.

[67] Inoue H, Kishimoto K, and Shibuya T (1996), Experimental wavelet

analysis of flexural waves in beams, *Exp. Mech.* **36**, 212–217.
[68] Kishimoto K, Inoue H, Hamada M, and Shibuya T (1995), Time-frequency analysis of dispersive waves by means of wavelet transform, *ASME J. Appl. Mech.* **62**, 841–846.
[69] Ohkami Y and Tanaka H (1997), Estimation of impact force and its location exerted on spacecraft (in Japanese), *Trans. Jpn. Soc. Mech. Eng., Ser. C.* **63C**, 4246–4252.
[70] Gaul L and Hurlebaus S (1998), Identification of the impact location on a plate using wavelets, *Mech. Syst. Signal Process.* **12**, 783–795.
[71] Briggs JC and Tse MK (1992), Impact force identification using extracted modal parameters and pattern matching, *Int. J. Impact Eng.* **12**, 361–372.

SUPPLEMENTAL BIBLIOGRAPHY

Antunes J, Paulino M, and Piteau P (1998), Remote identification of impact forces on loosely supported tubes: Part 2—Complex vibro-impact motions, *J. Sound Vib.* **215**, 1043–1064.
Arai M, Nishida T, and Adachi T (2000), Identification of dynamic pressure distribution applied to the elastic thin plate, *Inverse Problems in Engineering Mechanics II (Int Sym Inverse Problems in Eng Mech 2000, Nagano, Japan)*, Elsevier, 129–138.
De Araüijo M, Antunes, J, and Piteau P (1998), Remote identification of impact forces on loosely supported tubes: Part 1—Basic theory and experiments, *J. Sound Vib.* **215**, 1015–1041.
Johnson CD (1998), Identification of unknown, time-varying forces/moments in dynamics and vibration problems using a new approach to deconvolution, *Shock Vib.* **5**, 181–197.
Ma CK, Tuan PC, Lin DC, and Liu CS (1998), A study of an inverse method for the estimation of impulsive loads, *Int. J. Syst. Sci.* **29**, 663–672.
Ohkami Y and Tanaka H (1998), Improvement of impact force estimation exerted on spacecraft and its accuracy (in Japanese), *Trans. Jpn. Soc. Mech. Eng., Ser. C* **64C**, 2019–2025.
Paulino M, Antunes J, and Izquierdo P (1999), Remote identification of impact forces on loosely supported tubes: Analysis of multi-supported systems, *ASME J. Pressure Vessel Technol.* **121**, 61–70.
Rao Z, Shi Q, and Hagiwara I (1999), Optimal estimation of dynamic loads for multiple-input system, *ASME J. Vibr. Acoust.* **121**, 397–401.
Sundin KG and Ährström, BO (1999), Method for investigation of frictional properties at impact loading, *J. Sound Vib.* **222**, 669–677.
Tsuji T, Kawada Y, Suzuki Y, Yamaguchi T, and Noda N (1999), Identification of an impact force by radiated sound from the impacted body (Non-contact measuring experiments of the identification by the inverse analysis) (in Japanese), *Trans. Jpn. Soc. Mech. Eng., Ser. A* **65A**, 701–707.

Hirotsugu Inoue *received his BEng, MEng, and DEng degrees in mechanical engineering from Tokyo Institute of Technology in 1985, 1987, and 1993, respectively. He worked as a research associate of Tokyo Institute of Technology from 1987 before being promoted to an associate professor there in 1996. He stayed at the University of Manchester Institute of Science and Technology, UK and Ecole Polytechnique, France as a visiting researcher in 1998. His current research interests include inverse analyses in the mechanics of materials, wavelet analysis of elastic waves for ultrasonic nondestructive testing of materials, and impact durability of mobile electronic tools.*

John J Harrigan *is a Lecturer in the Department of Mechanical, Aerospace, and Manufacturing Engineering at the University of Manchester Institute of Science and Technology (UMIST). He received his BEng in Mechanical Engineering from the University of Sheffield in 1991 and his PhD from UMIST in 1995. After working as a Research Associate at UMIST, he was made a Temporary Lecturer in 1999 and a Lecturer in 2000. He is a member of the Impact and Explosion Engineering Group, and has published papers on inertia effects in impact energy absorbing structures and materials, as well as accurate measurement of impact force signals.*

Stephen Robert Reid *is the Conoco Professor of Mechanical Engineering in the Mechanical, Aerospace and Manufacturing Engineering Department at UMIST, where he heads the Applied Mechanics Division and the Impact and Explosion Engineering Group (IMPEX). He received his BSc (1966) and PhD (1969) degrees in Mathematics from the University of Manchester and MA (1977) and ScD (1991) degrees from the University of Cambridge. He has held appointments in the universities of Cambridge and Aberdeen. His main research interests include dynamic structural plasticity, fibre-reinforced composites and cellular materials. He has published over 175 papers and has been the Editor-in-Chief of the International Journal of Mechanical Sciences since 1987.*